CrossMark

Riding against the wind: a review of competition cycling aerodynamics

Timothy N. Crouch[1] · David Burton[1] · Zach A. LaBry[2] · Kim B. Blair[3]

Abstract Aerodynamics has such a profound impact on cycling performance at the elite level that it has infiltrated almost every aspect of the sport from riding position and styles, equipment design and selection, race tactics and training regimes, governing rules and regulations to even the design of new velodromes. This paper presents a review of the aspects of aerodynamics that are critical to understanding flows around cyclists under racing conditions, and the methods used to evaluate and improve aerodynamic performance at the elite level. The fundamental flow physics of bluff body aerodynamics and the mechanisms by which the aerodynamic forces are imparted on cyclists are described. Both experimental and numerical techniques used to investigate cycling aerodynamic performance and the constraints on implementing aerodynamic saving measures at the elite level are also discussed. The review reveals that the nature of cycling flow fields are complex and multi-faceted as a result of the highly three-dimensional and variable geometry of the human form, the unsteady racing environment flow field, and the non-linear interactions that are inherent to all cycling flows. Current findings in this field have and will continue to evolve the sport of elite cycling while also posing a multitude of potentially fruitful areas of research for further gains in cycling performance.

Keywords Aerodynamics · Bluff body · Sports · Cycling · Wind tunnel · CFD

✉ Timothy N. Crouch
timothy.crouch@monash.edu

David Burton
david.burton@monash.edu

Zach A. LaBry
zach.labry@gmail.com

Kim B. Blair
blairk@mit.edu

[1] Department of Mechanical Engineering, Monash University, Clayton, VIC 3800, Australia

[2] ATA Engineering, Inc., El Segundo, CA 90245, USA

[3] Massachusetts Institute of Technology and STI&E Consulting, Cambridge, MA, USA

1 Introduction

This year, elite cyclists from all around the world will have gathered to compete in one of cycling's greatest road races, the Tour de France. In a quiet moment, these athletes may reflect on their journey to Paris. For all, this journey will have required years of intense coaching, training and sacrifice, and for many cyclists this will have included hours in a wind tunnel searching for the optimal aerodynamic position and racing strategy. The clothes that the athletes will wear, the equipment the teams select, and the bicycles they ride will all have been developed with aerodynamics front of mind. The athletes will know that the difference between a podium and a respectable finish may be holding their form and position through the pain barrier, as to break form will increase the aerodynamic loads they must fight to overcome—at which point they will be riding against the wind.

In this review paper, we aim to explain the current understanding of the aerodynamics of competitive track and road cycling and identify areas where further research is required. It is clear that aerodynamic performance can be as fundamental to success as power production. However, the application of the aerodynamics principles presented is not limited to competition. Today, cycling is an important

and sustainable means of transport, a fitness and recreational activity, a competitive sporting pursuit, a spectator sport with a huge fan base, and an industry of growing economic significance. Aerodynamics is a factor in all these: whether it is the time taken for a cyclist to commute to work, the effort required to overcome a head-wind, time-trial success at the Tour de France, or product performance and differentiation.

## 1.1 Aerodynamics and the evolution of the 1-h record

No other human-powered transport mechanism has had as wide an uptake and impact on our society as the bicycle. Perhaps surprisingly, the modern bicycle has existed in similar form since the mid- to late 19th century, with recent technological advances driven mostly by uptake from other industries (e.g. materials such as carbon fibre, manufacturing techniques, and numerical modelling) and competitive innovators. The bicycle likely developed from a merging of technologies from earlier sit astride push along velocipedes and treadled tri- and quadra-cycles. By the 1870s, cyclists were attempting to set records, both Englishman James Moore and American Frank Dodds are separately rumoured to have claimed the first hour record. Almost 150 years later, the 1-h time-trial remains a landmark record of human performance. The competition has recently been re-invigorated by the Union Cycliste Internationale (UCI) that is the international governing body of cycling relaxing the aerodynamic rules that previously restricted its advancement. In fact, the evolution of this record is explanatory of the critical role that aerodynamics plays in the performance of any competitive cyclist.

Figure 1 shows the advancement of the world hour record between 1900 and 1993, which was almost linear. Recent development of the hour record can be traced back to 1972 when Eddy Merckx, taking advantage of the lower air density at altitude in Mexico City, set a record of 49.4 km. The record stood until 1984 when broken by Francesco Moser using a skin suit and disc wheels. However, the greatest period of change commenced in 1993 when Scottish cyclist Graeme Obree ("the flying Scotsman") rode an innovative homemade bicycle to a new record. The bicycle set-up allowed him to ride with his head down and hands tucked in underneath his chest, known as the 'Obree position'. A dramatic period of development ensued with competitors adopting different extreme positions all aimed at minimising aerodynamic drag. This period culminated with Chris Boardman's 1996 world record achieved riding the "superman position"—a record that remains the "best human effort" record today. Following Boardman's record, the UCI, which were struggling with the definition of the bicycle, regulated to prevent these extreme positions by dividing the records into separate "best human effort" and "world record" categories depending upon the equipment used. As a result these distances were no longer attainable. In 2014, the UCI relaxed the rules on the bicycle and equipment to allow the use of technologies currently available in endurance track events, leading to another rapid increase in the hour record now known as the "unified hour record". In this case, the sudden increase was not caused by rapid technology advancement, rather a correction for new technology developed over the period when banned.

Despite the piecemeal aerodynamic advance of the conventional bicycle evident through the evolution of the 1-h record, it is important to realise that the aerodynamics of a conventional bicycle are far from optimal. It is for this reason that the opportunities for improvement are so great. This is highlighted by comparison of the human-powered vehicle (HPV) 1-h record, which is essentially a faired recumbent bicycle, to that of the conventional bicycle. The

Fig. 1 Progression of the hour record categories from when the hour record was initiated in 1983 to the present [1]. The current hour record (unified UCI rules) of 54.526 km was set by Bradley Wiggins on the 7 of June 2015 London
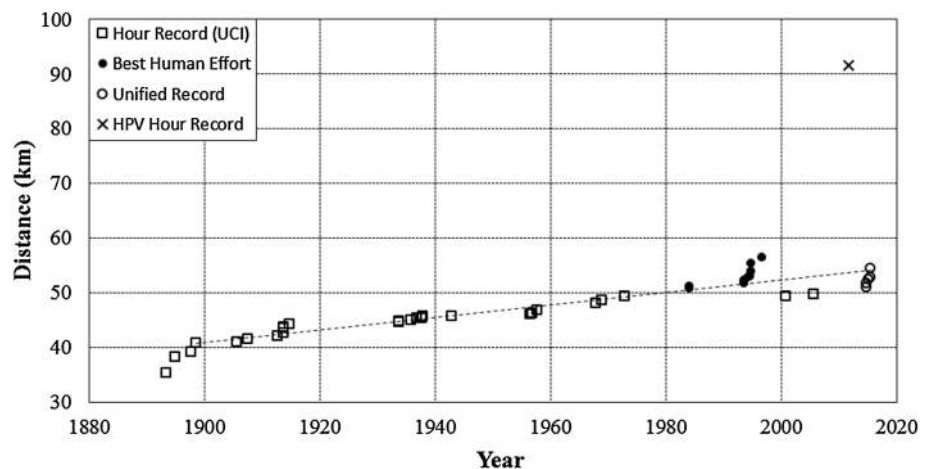
current HPV record is over 90 km, nearly double that of Boardman's best human effort record (56.375 km) and Wiggins' one-hour record (54.526 km).

1.2 Aerodynamics and cyclist performance

The fundamental physics governing the motion of a cyclist are well known and have been modelled in the literature. Martin et al. [2] validated a mathematical model for cycling power. The power input from the rider 'P_{Total}' is transferred from the crank to the wheels by the chain with an efficiency, 'E'. The model accounts for aerodynamic resistance 'P_{AT}', rolling resistance 'P_{RR}' from the resistive force between tyre and road, wheel bearing friction losses 'P_{WB}', potential energy 'P_{PE}' changes due to riding up or down hill, and inertial/kinetic energy 'P_{KE}' changes arising from linear (cyclist forward speed) and rotational acceleration:

$$P_{\text{Total}} = \frac{P_{\text{AT}} + P_{\text{RR}} + P_{\text{WB}} + P_{\text{PE}} + P_{\text{KE}}}{E}. \tag{1}$$

Aerodynamic power can be attributed to two main components: the resistive force acting against the direction of motion of the cyclist (aerodynamic drag) and the aerodynamic forces (or more correctly moments) that resist the rotation of the wheels:

$$P_{\text{AT}} = P_{\text{A}} + P_{\text{AR}}, \tag{2}$$

where 'P_{A}' is the linear component and 'P_{AR}' is the rotational component. The aerodynamic drag force 'F_{D}' experienced by a cyclist:

$$F_{\text{D}} = C_{\text{D}} \cdot A \frac{1}{2}\rho U^2, \tag{3}$$

is a function of the drag coefficient 'C_{D}' and the frontal area of the cyclist 'A'. It increases linearly with air density 'ρ'; low air density and consequently lower aerodynamic drag are the reasons that so many world records have been set at high altitude. Air density of dry air varies as a function of pressure 'p', temperature 'T', and a specific gas constant 'R_{S}':

$$\rho = \frac{p}{R_{\text{S}}T}. \tag{4}$$

The drag force also increases with the square of the relative wind speed 'U', as a corollary the power required to overcome these forces increases with the cube of the wind speed:

$$P_{\text{A}} = F_{\text{D}} \cdot U = C_{\text{D}} \cdot A \frac{1}{2}\rho U^3. \tag{5}$$

Aerodynamics becomes increasingly dominant over other forces as speed increases. To increase performance, especially in events where inertial changes (acceleration) are not significant, a cyclist must either increase the power they produce or decrease their resistance. Kyle and Burke [3] found that aerodynamic resistance accounts for over 90% of resistance a cyclist encounters on a flat surface, and Martin et al. [2] found that aerodynamic resistance accounted for between 56 and 96% of power depending on road gradient. This creates an exciting circumstance where smaller, less powerful athletes can compete against larger stronger cyclists by optimising their interaction with the fluid medium (i.e. the air).

1.3 Aerodynamic forces and moments

A cyclist experiences six direct aerodynamic actions (three forces and three moments), as shown in Fig. 2. In addition
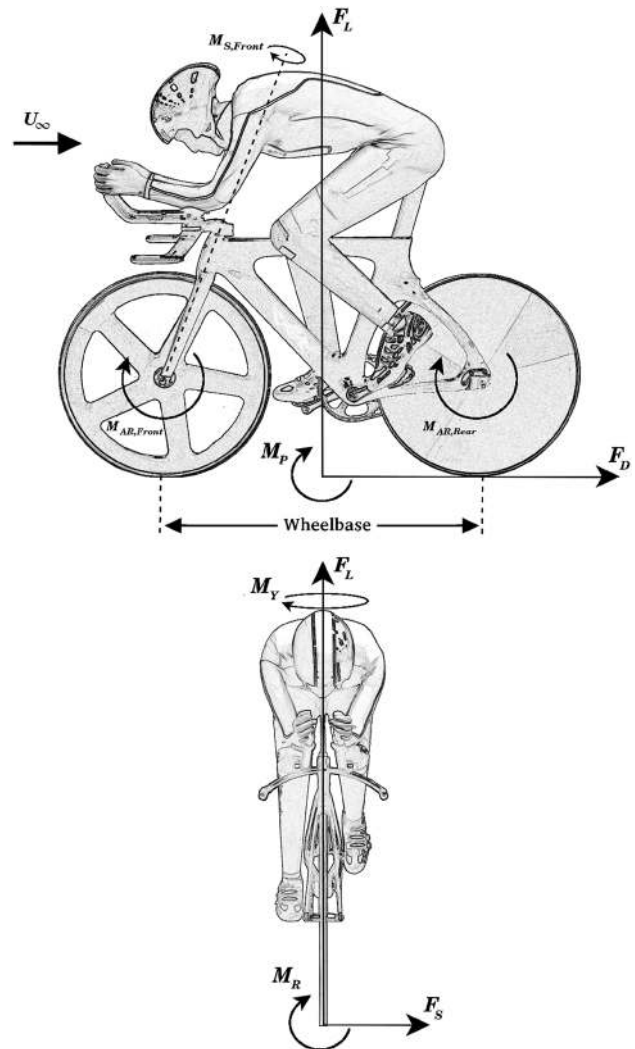

Fig. 2 Digram showing cyclist and bicycle aerodynamic forces (F_{L}, F_{D}, F_{S}) and moments (M_{P}, M_{R}, M_{Y}) about the centre of the wheelbase, along with steering and aerodynamic moments acting on the wheels

to the drag force that acts in the opposite direction to cyclist's motion, the other aerodynamic force components consist of a side force 'F_S', and the vertical lift force 'F_L'. The moments are defined about the centre of the wheelbase as a pitching moment that acts to lift the front wheel 'M_P', roll moment 'M_R', and yaw moment 'M_Y'. All these forces and moments can be described as force 'C_F' and moment 'C_M' coefficients, normalised by the frontal area and dynamic pressure, and in the case of moment coefficients by the frontal area and the wheelbase of length 'l':

$$C_{F:D,S,L} = \frac{F_{D,S,L}}{\frac{1}{2}\rho U_\infty^2 A},$$ (6)

$$C_{M:P,R,Y} = \frac{M_{D,S,L}}{\frac{1}{2}\rho U_\infty^2 Al}.$$ (7)

In addition, the bicycle and cyclist experience indirect resistance to rolling and pedalling motion, through aerodynamic resistance to wheel (and leg) rotation '$M_{AR,Front}$' and '$M_{AR,Rear}$'. Finally, a steering moment '$M_{S,Front}$' is experienced on the front wheel that acts about the front fork axis and thereby can affect steering and stability in cross-wind, especially in the case of a front disc wheel.

2 Fluid dynamics of cycling

2.1 Bluff body aerodynamics

Flows around a cyclist exhibit large regions of separation and, therefore, fall into the category of bluff bodies. In contrast to streamlined bodies such as aerofoils, which have rounded leading edges and a gradual reduction in body width and cross-sectional area from the widest point of the body to the trailing edge, a bluff body has sharp edges or a much more dramatic reduction in body width towards the trailing surfaces [6]. This type of geometry results in large adverse pressure gradients imposed on the boundary layer that are too large to sustain attached flow. As a result, bluff body flows are characterised by large regions of separated flow that may or may not reattach to the surface.

Unlike streamlined bodies, where the viscous tangential wall shear stress forces contribute the largest proportion to aerodynamic drag, the aerodynamic resistance in cycling is mainly from pressure drag [8]. Flow separation around cyclists results in the formation of a turbulent wake and large-scale low-pressure vortices as depicted in Fig. 3. The magnitude of the pressure drag is proportional to the pressure differential generated between the low-pressure wake areas and the high-pressure stagnation regions located on the leading surfaces of the rider [9]. The resultant pressure force is found by integrating the surface pressure
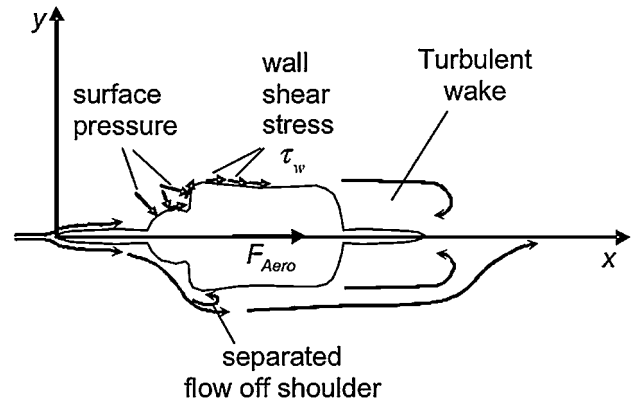

Fig. 3 Simplified diagram of the flow field around a cyclist from Martin et al. [9], highlighting the high-pressure leading surface regions and the low-pressure turbulent wake. Reprinted with permission from Human Kinetics, Inc., from Martin et al. [9], ©1999; permission conveyed through Copyright Clearance Center, Inc.

distribution, which acts normal to the body surface, over its entire surface.

The drag coefficient, introduced in Eq. 6, describes the aerodynamic efficiency of a body independent of the size of the shape. In cycling, for a given rider position (and hence frontal area), the aim is to minimise the drag coefficient and thereby the resistive forces. It depends on a number of factors including body shape, orientation, surface roughness, free-stream flow conditions ,and Reynolds number 'Re'. Re represents the ratio of inertial to viscous forces:
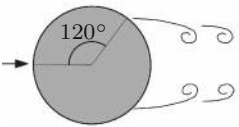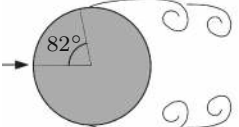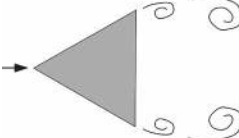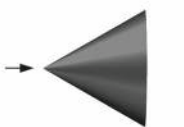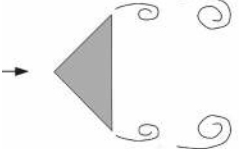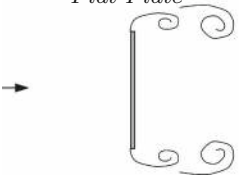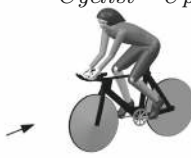
$$Re = \frac{U_\infty x}{\upsilon},$$ (8)

where 'x' is the characteristic length scale and 'υ' is the kinematic viscosity.

Table 1 presents the drag coefficients for a range of shapes and vehicles. Typically, the drag coefficient of a cyclist ranges from ≈0.6 for a streamlined time-trial position to >0.8 for an upright position. In this case, the more efficient time-trial position has the added benefit of a lower frontal area. From a fluids perspective, a cyclist and bicycle is not a very aerodynamic geometry. Using fairings to shield the body from the flow, such as those used in the designs of high-speed human-powered vehicles, the drag coefficient of a cyclist can be reduced by more than 80% with drag coefficients of the order of ≈0.1.

Due to the majority of aerodynamic drag in cycling resulting from pressure forces, the largest gains in aerodynamic performance are achieved by rider positions, equipment, and tactics that reduce the pressure differential between the leading and trailing edge surface of the rider–bicycle system and the effective area over which the pressure differential acts on in the drag-producing direction. This is achieved either by minimising the frontal area, increasing the pressure on rearward facing surfaces

Table 1 Drag coefficients of simple 2D, 3D, and more complex 3D geometries for a range of Reynolds numbers [4–7]

2-D Geometry		3-D Geometry		Complex 3-D Geometry	
Airfoil	$x = chord\ (c)$ $A = c(b)$ $Re \approx 1 \times 10^5$ $C_D \approx 0.1$	*Elipsoid*	$x = diameter\ (d)$ $A = \frac{\pi}{4}d^2$ $Re \approx 1 \times 10^5$ $C_D \approx 0.05$	*Faired − HPV*	$x = \sqrt{A}$ $A = frontal$ $Re \approx 1.5 \times 10^6$ $C_D \approx 0.07$
Cirular Cylinder (120°)	$x = diameter\ (d)$ $A = d(b)$ $Re \approx 5 \times 10^5$ $C_D \approx 0.4$	*Sphere*	$x = diameter(d)$ $A = \frac{\pi}{4}d^2$ $Re \approx 5 \times 10^5$ $C_D \approx 0.1$	*Fast − Back Car*	$x = \sqrt{A}$ $A = frontal$ $Re \approx 4 \times 10^6$ $C_D \approx 0.28$
Cirular Cylinder (82°)	$x = diameter\ (d)$ $A = d(b)$ $Re \approx 1 \times 10^4$ $C_D \approx 1.2$	*Sphere*	$x = diameter\ (d)$ $A = \frac{\pi}{4}d^2$ $Re \approx 1 \times 10^4$ $C_D \approx 0.5$	*Small Bus*	$x = \sqrt{A}$ $A = frontal$ $Re \approx 3.5 \times 10^6$ $C_D \approx 0.42$
60° *Wedge*	$x = width\ (w)$ $A = w(b)$ $Re \approx 1 \times 10^5$ $C_D \approx 1.4$	60° *Cone*	$x = diameter\ (d)$ $A = \frac{\pi}{4}d^2$ $Re > 1 \times 10^4$ $C_D \approx 0.8$	*Cyclist − Time Trial*	$x = \sqrt{A}$ $A = frontal$ $Re \approx 7 \times 10^5$ $C_D \approx 0.60$
90° *Wedge*	$x = width\ (w)$ $A = w(b)$ $Re \approx 1 \times 10^5$ $C_D \approx 1.6$	90° *Cone*	$x = diameter\ (d)$ $A = \frac{\pi}{4}d^2$ $Re > 1 \times 10^4$ $C_D \approx 1.15$	*Semi − Trailer*	$x = \sqrt{A}$ $A = frontal$ $Re \approx 6 \times 10^6$ $C_D \approx 0.70$
Flat Plate	$x = width\ (w)$ $A = w(b)$ $Re \approx 1 \times 10^5$ $C_D \approx 2.0$	*Disk*	$x = diameter\ (d)$ $A = \frac{\pi}{4}d^2$ $Re > 1 \times 10^3$ $C_D \approx 1.1$	*Cyclist − Upright*	$x = \sqrt{A}$ $A = frontal$ $Re \approx 7 \times 10^5$ $C_D > 0.80$

Geometries are depicted from streamlined to increasing bluffness working down the table from top to bottom. The aerodynamic efficiency and the degree to which a geometry is streamlined are strongly dependent on body shape. The wake width is depicted for 2D bodies demonstrating the trend that the degree of 'bluffness' increases with increasing wake width (relative to the characteristic length scale x). We also note that for geometries exhibiting smooth curves (such as cylinders and spheres) the drag coefficient is dependent on the Reynolds number. Note 'b' represents the span of the body

and in the wake, or by reducing the magnitude of the high-pressure stagnation regions on the leading surfaces of the body.

Prior to separation, the surface pressure is well approximated using potential flow theory. For steady irrotational flows, ignoring gravity effects, the local static pressure 'P_S' around a body can be approximated using Bernoulli's equation:

$$P_T = P_S + \frac{1}{2}\rho U^2, \qquad (9)$$

where 'P_T' represents the total pressure (equal to pressure at stagnation points on the body) and U is the local fluid

velocity. From this equation, it can be seen that the regions of high velocity correspond to low static pressure and regions of low velocity correspond to high static pressure. Near forward-facing surfaces, large regions of flow stagnation/low velocity are to be avoided and hence curved surfaces are favoured. On rearward surfaces, the aim is to decrease the flow speed, increasing pressure, without causing separation. Unfortunately, the flow is inclined to separate under positive (adverse) pressure gradients meaning that any expansion to reduce flow velocity must be gradual, which is one reason low drag shapes tend to have long tails. It follows that maintaining attached flow and minimising the size of the wake or controlling the location at which flow separation occurs is one of the primary objectives in the design of cycling equipment or optimising riding position for aerodynamic performance. The prediction of the location at which flow separation will occur is often difficult as it depends on both the characteristics of the upstream boundary layer and flow structures in the near wake [10].

The nature of the boundary layer describing the velocity profile of the fluid near the surface of a moving body is dependent on the body geometry and surface texture as well as the freestream air properties. Compared to laminar boundary layers, which have only diffusive intermixing, turbulent boundary layers are characterised by intense small-scale eddies that transfer momentum from the freestream to the viscous interface at the body's wall [11]. The increased momentum at the body's surface gives turbulent boundary layers a greater ability to overcome adverse pressure gradients compared to laminar boundary layers. As a result, turbulent boundary layers are less susceptible to flow separation over curved surfaces leading to reductions in the pressure drag acting on bluff bodies.

2.2 Cyclist wake structure and major flow regimes

The approach to minimising aerodynamic drag is greatly complicated when separation occurs and even more so in the case of complex three-dimensional geometries (e.g., a cyclist). The flow over a cyclist is further complicated when the unsteady aerodynamics associated with the motion of the legs around the crank cycle is considered. Recently, there has been a considerable amount of work using both experimental and numerical techniques to locate where the flow separates from the body of the rider over the course of the pedal stroke and how the three-dimensional aspects of the flow relate to the aerodynamic forces acting on cyclists.

Experimental studies by Crouch et al. [12, 13] and numerical investigations by Griffith et al. [14] have recently provided insight into the nature of the flow and the origin of the aerodynamic forces at play for cyclists. These studies utilised a full-scale mannequin in a time-trial position, and a numerical cyclist model of a similar geometry to visualise and quantify the development of the large-scale flow structures that develop in the wake over the course of a pedal stroke. A quasi-steady analysis, whereby the flow was analysed for a series of static leg positions around a full 360° pedal stroke, revealed that the aerodynamic drag of a cyclist varies significantly (≈20%) as a function of crank angle. The dependence of aerodynamic drag on crank angle was first reported on by Kyle et al. [15], who observed similar variations in the aerodynamic drag force between a horizontal and a vertical crank position. Measurements of the frontal area of the mannequin and the bike varied by less than 2% over a full pedal cycle and led the authors to conclude that the majority of the variation in drag with leg position must arise from variations in the drag coefficient, which depends on the structure of the wake.

The link between the large variation in the aerodynamic drag force and the state of the flow in the wake was made from detailed wind tunnel wake velocity field surveys, surface pressure measurements, and flow visualisation studies. From velocity fields measured for various cross-sections in the wake, two major flow regimes were identified along with the large-scale flow structure variants as the legs progressed around the crank cycle. These are shown in Fig. 4 and consist of a symmetrical low-drag flow regime for crank angles close to the horizontal and an asymmetrical high-drag flow regime which occurred when one leg was raised and the other in an extended position. The symmetrical regime consisted of streamwise vortices (vortex cores aligned with the freestream direction) that originate from the upper and inner thighs when the cranks were close to the horizontal position. The asymmetrical high-drag regime consisted of a pair of intense counter-rotating streamwise vortices that persist far into the downstream wake. These originate when the flow separates from the upper hip of the extended leg and the rear of the hip of the raised leg for leg positions closer to a vertical crank angle.

The variation in the aerodynamic drag force that occurs throughout the crank cycle was found to be correlated with changes to the size and strength of the large-scale flow structures. Time-averaged surface pressure measurements and skin friction flow visualisations performed on the back and base of the mannequin showed that the primary flow structures were responsible for the large low-pressure regions that develop on a cyclist's back. These low-pressure regions, shown in Fig. 4c, were found to account for 12–20% of the total aerodynamic drag force throughout the crank cycle. Over 60% of the variation in drag with leg position could be accounted for solely by the large change in the pressure distribution on the back and hips throughout
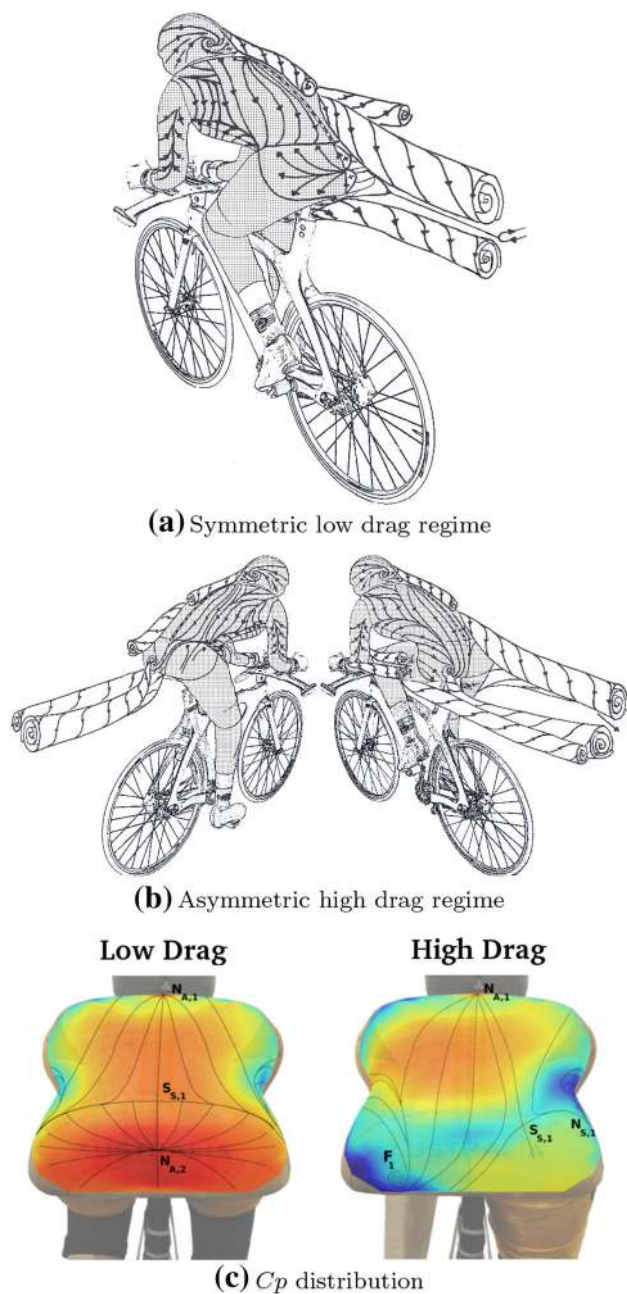
(a) Symmetric low drag regime

(b) Asymmetric high drag regime

Low Drag   High Drag

(c) C_p distribution

Fig. 4 Flow topology of streamwise vortex system for **a** symmetric low-drag flow regime and **b** asymmetric high-drag regime viewed from the right-handed and left-handed perspectives. **c** Surface pressure distributions for each low- and high-drag flow regime. Contours of the surface pressure coefficient C_p range $-0.8 \leq C_p \leq 0$ for colours *blue* (low-pressure regions) to red (high pressure), from Crouch et al. [12] (colour figure online)

the crank cycle. These findings have also been supported by recent studies that include the dynamic motion of the legs for realistic racing cadences [13, 16, 17]. These studies show that the large-scale wake structures identified in quasi-steady experiments are still the dominant flow features at elite-level time-trial speeds and cadences. The limit at which a quasi-steady assumption will no longer be

representative of dynamic pedalling scenarios, which one would expect to occur at a higher pedalling speed-to-forward riding speed ratio than currently studied, remains unknown.

3 Methods of investigating cycling aerodynamics

3.1 Wind tunnels

The wind tunnel is a pivotal tool for the further development and assessment of cycling aerodynamics. Although most wind tunnel facilities used for cycling aerodynamics have their backgrounds in the automotive and aerospace industries, some bicycle manufacturers have developed their own wind tunnels for cycling aerodynamics [18]. Wind tunnels offer a controlled repeatable wind environment that can be tuned for a wide range of cycling conditions and generated on demand. This enables detailed test programmes to be carried out utilising high-fidelity wind tunnel measurement systems. Flows around cyclists are simulated in a wind tunnel, where cyclists are at rest relative to the wind tunnel and air is blown over them to simulate wind conditions experienced by cyclists on the road or track. In this frame of reference to match road conditions, a moving floor or a ground plane would be required. Although wind tunnels with moving floors are widely used and are critical to automotive and racing car aerodynamics, simulating a moving floor is less of an issue for cycling aerodynamics as the vast majority of the bicycle–rider system volume is situated away from the floor, and provided that measures are taken to limit the boundary layer growth, a stationary floor will have only a small effect on the large-scale flow field. This, however, is not true for components of the bicycle such as the wheels, which are located in the boundary layer.

Most wind tunnels are designed for low-freestream turbulence levels and a uniform velocity distribution in the test section. As a result, wind tunnels offer a simplification of real cycling environments. On-road and track flows are dictated by factors such as turbulent atmospheric boundary layers, air currents driven by temperature gradients, the wind direction, and the turbulent wakes of other bodies [19, 20]. Fluid mechanical processes such as flow separation and the transition to turbulence can be influenced by freestream turbulence levels, flow uniformity, flow angularity, and pressure gradients in the test section. Currently, there are no standard wind tunnel test conditions for the aerodynamic evaluation of cyclists.

Typical wind tunnels used for cycling include both closed return (*Göttingen* type) and open non-return (*Eiffel* type) circuits employing either fully closed (walls surrounding test section) and open test sections (usually 3/4

open variety, whereby a jet of air is generated by a nozzle blowing over a ground plane as shown in Fig. 5). Both types of test sections offer advantages and disadvantages when simulating flows around cyclists referenced to an infinite flow or 'free-air' case (riding in an open environment with still air). One of the main differences between the two designs is how the flow in the test section is altered compared to free-air conditions. In fully closed test sections, the wind tunnel walls restrict the displacement of the streamlines around the cyclists. One effect of this is that the local air velocity around the cyclist is increased and can have a significant effect on aerodynamic force and pressure coefficients.

In open-jet facilities, the blockage effects tend to be less; however, the correction methods are more complex. For example, the curvature of the jet boundary is increased or over-expanded, resulting in a lower velocity profile around the cyclist. Blockage corrections have been developed for both closed and open-jet test sections that take into account the solid blockage and wake blockage effects [21–24]. One of the key parameters to the corrections is the blockage ratio given as the ratio of the frontal area to the area of the wind tunnel cross-section. It is recommended that blockage ratios be <5%; however, this is only a guideline and open-jet facilities are much less susceptible to solid blockage effects. Open-jet facilities are more prone to additional influences however known as jet/collector blockage and horizontal buoyancy forces that result from static pressure gradients that develop across the test section. Particularly, when testing high blockage, long models, or large cycling arrangements (drafting cyclists in a pace-line formation for

example), blockage effects and the type of wind tunnel facility must be considered and taken into account when interpreting findings.

3.2 Wind tunnel measurement techniques

The most common measurement performed with cyclists in the wind tunnel is the time-averaged aerodynamic force measurements. The purpose is usually to measure the effect of different rider positions and cycling equipment configurations (see Table 4 which is discussed in Sect. 4.1 and presents a range of cycling wind tunnel investigations). Typically, this involves positioning the bicycle on a force balance that is housed underneath the wind tunnel floor via struts connected to the wheel axles. The force balance is typically mounted on a turntable that facilitates the yawing of the rider and system relative to the wind to understand changes in aerodynamic forces associated with cross-wind. The bicycle is sometimes installed on a raised platform that incorporates a splitter plane extending forward of the balance to limit the impact of the wind tunnel floor boundary layer on force measurements. Early wind tunnel testing of cyclists involved force measurements of cyclists holding stationary, non-pedalling positions. Nowadays, it is more common to measure aerodynamic forces with the cyclists pedalling and the wheels rotating, which provides a better representation of road/track cycling conditions. The rotation of the wheels has been achieved using mechanical roller/belt drives [8] and systems utilising electric motors [2]. The same approach can be taken to measure the forces on a bicycle, in the absence of a cyclist. Care needs to be
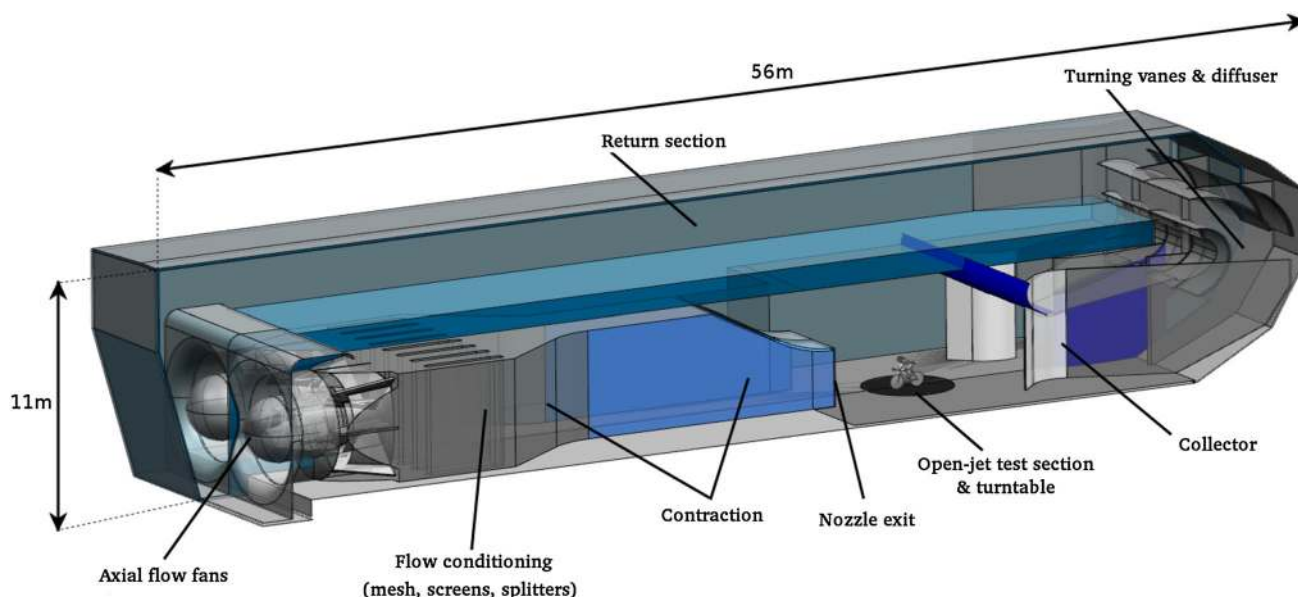

Fig. 5 Cutaway of a 3/4 open-jet wind tunnel (Monash University Clayton Campus) which is ideal for full-scale testing of athletes (note: there are many configurations and designs of open-jet wind tunnels; this is just one example)

taken in comparing results from wind tunnel measurement of bicycle drag. In the authors' experience, small effects such as pedal type and position, seat treatment, and small misalignments can all affect drag measurements of a bicycle alone but are unlikely to be significant to the combined drag of bicycle and cyclist. This is important when comparing the relative performance of different bicycles.

Often aerodynamic forces measured in a wind tunnel are not reported as coefficients, which require measurements of the projected frontal area, but as drag area measurements 'C_{DA}'. The drag area given by

$$C_{DA} = \frac{D}{\frac{1}{2}\rho U_\infty^2} \tag{10}$$

provides a means of eliminating the uncertainty associated with measuring the frontal surface area [2, 4], while still providing a way of standardising force measurements for variations in fluid properties and velocity between wind tunnel tests. As aerodynamic drag is dependent on both the drag coefficient and the frontal area, the drag area also dictates the aerodynamic power requirements of riders to maintain a given speed and serves as a performance measure. When force coefficients are reported, the frontal area has been determined using a number of techniques that have been summarised by Debraux et al. [28]. These methods usually involve photographs recorded from the frontal views of rider position that are analysed using digital image processing techniques or the weighing of photographs technique [29–31].

One of the major problems with athlete wind tunnel measurements is the repeatability of rider position. The validity of assigning forces and any aerodynamic quantity associated to a particular rider shape and position depends upon the ability of the rider to maintain their position throughout the testing period. Further, many testing scenarios require the rider to dismount from the bicycle in the wind tunnel and re-mount the bicycle in the same position. Small variances in rider position also result in a change in the physical geometry of the rider, making it difficult to isolate exactly what variables are influencing aerodynamic force measurements of rider position. In an effort to control for rider positioning, some wind tunnels have implemented camera and motion tracking systems to monitor and record the position of athletes throughout testing.

By performing wind tunnel experiments on a mannequin, rider positions can be accurately repeated and maintained for extended periods of time and tested on demand. Testing with mannequins also allows for the geometry and position to be decoupled. Cycling mannequins are increasingly being used both in fundamental research and industry for detailed wind tunnel investigations. Testing with cycling mannequins opens up additional wind tunnel testing methods that are impractical or simply cannot be performed with athletes. Velocity field, surface pressure, and flow visualisation measurement techniques provide additional information on the nature of the aerodynamic forces acting on cyclists. Detailed knowledge of the link between the flow field, surface pressure distributions, and the aerodynamic forces is critical to our understanding of these flows, the further development and design of cycling equipment, and the validation of numerical codes. Figure 6 shows a small sample of some of these methods applied to cycling that utilise point velocity measurements with probes and particle image velocimetry (PIV), surface pressure systems, and flow visualisation techniques. For a detailed description of these methods and many more wind tunnel testing techniques, see Tropea et al. [6] and Barlow et al. [32].

3.3 Computational fluid dynamics

With improvements in meshing methods, increases in computing power, and advances in turbulence modelling and prediction of flow separation, computational fluid dynamics (CFD) is now capable of being practically utilised as another tool for investigating viscous flows around complex three-dimensional geometries such as a cyclist. As outlined in a review of the impact of CFD in sport by Hanna [33], CFD is being increasingly used to solve aerodynamics problems in sports ranging from car racing such as formula one, yacht racing, swimming, soccer, cricket, and cycling. In recent years, numerical codes have been used to simulate flows around bicycle components such as wheels [34, 35] and investigate the aerodynamics of different rider positions [27, 36].

There are many benefits to using CFD to investigate rider aerodynamics as it enables information about the flow field around a cyclist system to be obtained which would otherwise be extremely difficult or prohibitively time-consuming process to obtain experimentally. CFD has the potential to solve for the entire flow field that is resolved not only in space but in the time domain as well. Figure 7 shows the example numerical simulations of the flow field around cyclist geometries and bicycle components. Numerical simulations allow for the aerodynamic forces acting on a cyclist system to be decomposed into the viscous and pressure force components, which can be evaluated independently. In addition to the aerodynamic forces, information about body heat transfer rates and cooling can be gained from CFD [36]. Large parametric studies of the effect of position, equipment, and cross-winds to name a few can be performed by running multiple simulations in parallel. Using CFD, researchers can calculate the relative contribution to the overall drag of aerodynamic forces acting on specific parts of the cyclist system, such as the helmet, arms, torso, legs, and bicycle.
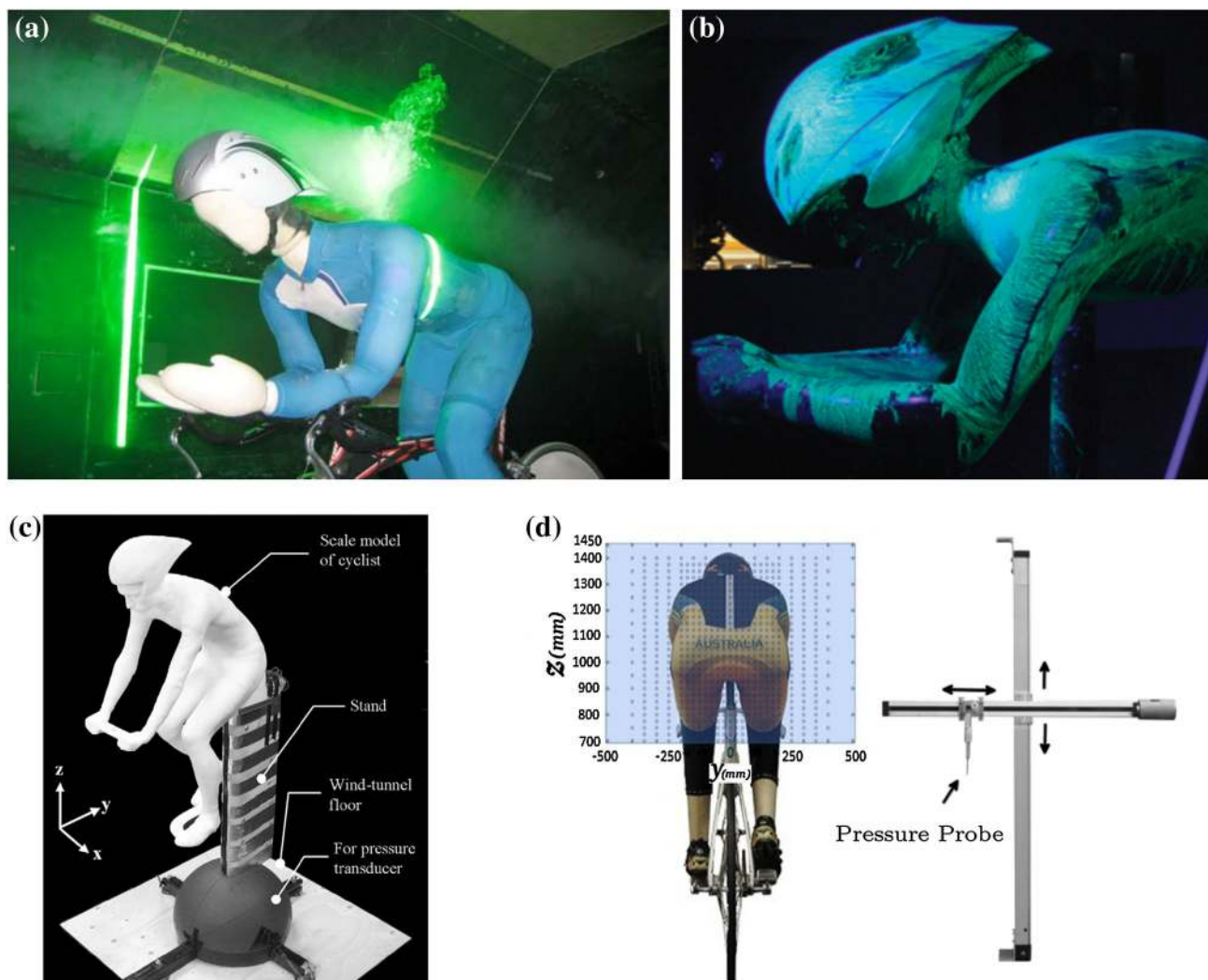
Fig. 6 **a** Measurements of the flow field in the wake of helmets using two-dimensional PIV by Chabroux et al. [25]. **b** Surface oil flow visualisations highlighting flow separation lines on the upper arm by Brownlie et al. [26]. Reprinted from Brownlie et al. [26], with permission from Taylor & Francis Ltd. (http://www.tandfonline.com). **c** A scale model cyclist manufactured using rapid prototyping methods for aerodynamic force and surface pressure measurements to validate numerical simulations by Defraeye et al. [27]. Reprinted from Defraeye et al. [27], pg 2283, ©2010, with permission from Elsevier. **d** Time-averaged three-component velocity fields measured in the wake of a mannequin using a two-axis motorised traverse to map the flow with a multi-hole pressure probe by Crouch et al. [12]

Table 2 shows the relative contribution to the aerodynamic drag force from various components of the bicycle and rider. Numerical simulations predict that for a streamlined position the bicycle contributes $\approx 20\%$ to the total aerodynamic resistance and aerodynamic forces acting on the body are dependent on the phase of the crank cycle the legs are positioned in.

The equations describing fluid motion are known as the Navier–Stokes Equations (NSE) which are based on conservation principles of mass, momentum, and energy. These equations contain all the necessary information to completely model the flow physics of problems as varied as the weather, ocean currents, and flows around cyclists. CFD simulations involve solving these equations over the flow field using a discretised spatial domain (known as a computational grid or mesh) and are solved either until a steady-state solution is achieved or in time increments or steps for unsteady or transient simulations. When solved directly through Direct Numerical Simulation (DNS), no averaging or simplifying assumptions are made. However, DNS comes at an extremely high computational cost. As DNS requires modelling all scales of turbulent motions in both space and time, extremely fine meshes and small time steps are required. This results from the fact that the mesh size required to capture all the flow physics scales with the ratio between the largest 'L' and the smallest 'l' turbulent scales which increases dramatically with Re ($L/l \sim Re^{9/5}$) [39].

For practical applications involving high Reynolds numbers and complex geometries, such as cyclists who operate at Re numbers orders of magnitude larger than what

Fig. 7 a A snapshot of a transient simulation showing the vortex wake structure of a numerical cyclist model holing a static time-trial positi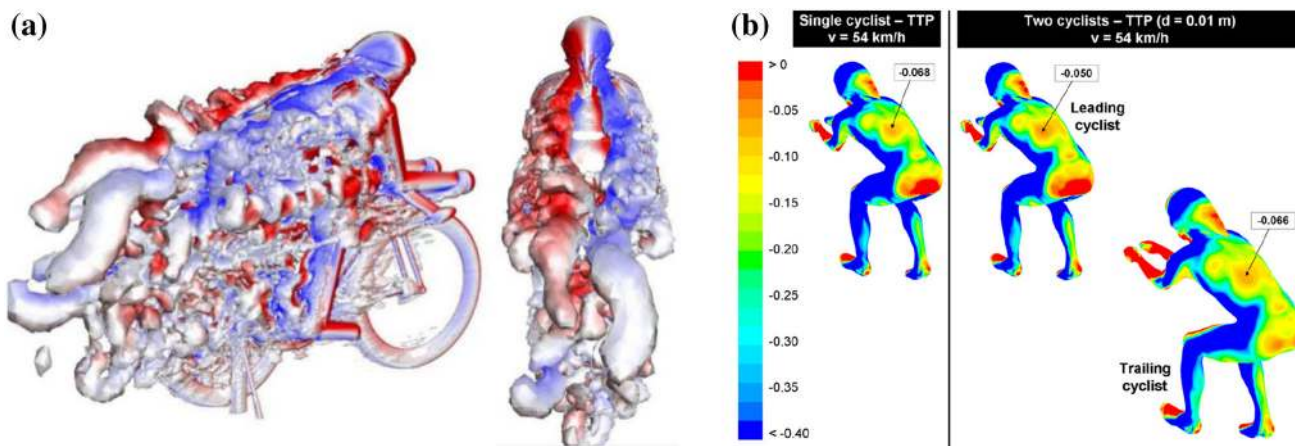on by Griffith et al. [14]. **b** Contours of the surface pressure coefficient around a single and drafting cyclist by Blocken et al. [37]. Reprinted from Blocken et al. [37], p 443, ©2012, with permission from Elsevier

Table 2 Relative contribution of various parts of the body and the bicycle to the total aerodynamic resistance

Study	Key variable	Simulation	Position	Crank	Head (%)	Arms (%)	Torso (%)	Left leg (%)	Right leg (%)	Bicycle (%)
[36]	Position	Steady-$k-\epsilon$	U, D, TT	0°	14–20	15–26	12–24	21–28	17–25	–
[38]	Multi-riders	Steady-$k-\epsilon$	TT	0°	7–16	22–24	7–14	21–30	27–35	–
[14]	Leg position	Steady-SST	TT	0°–180°	14–17	23–31	23–32	11–22	11–23	17–20

Cycling position is indicated by *U*, *D*, and TT which represent Upright, Down, and Time-Trial positions, respectively. Note that % given for Defraeye et al. [36, 38] do not include the bicycle and have been condensed for brevity. For a more detailed breakdown of the magnitude of the aerodynamic forces acting on the body, the reader is referred to these articles

can currently be solved using DNS, various averaging and turbulence modelling techniques must be utilised. One of the most common is various applications of the Reynolds Averaged Navier–Stokes equations (RANS). Instead of solving the NSE equations directly they are averaged and the time-averaged flow field is resolved. This averaging process requires the use of turbulence models to close the equations so that they can be solved. Various other modelling techniques also exist which blend solving the flow directly and using models such as Large Eddy Simulations (LES) and Detached Eddy Simulations (DES) where only the large turbulent motions are resolved in space and time and the influence of the small scales is modelled. As the outputs from CFD are sensitive to the initial input conditions, mesh size, time step size, turbulence models, and whether steady or transient simulations have been computed, the best outcomes, both in research and industry, arise when CFD is used in combination with an experimental test programme.

3.4 Combining computational and experimental methods

Paramount to the successful application of CFD in cycling is the means to ensure that numerical codes accurately capture the fundamental flow physics that determines the aerodynamics of the system being modelled. In order for computational fluid dynamics to progress in cycling, researchers and sports scientists must have confidence in results obtained from CFD simulations. The selection of appropriate turbulence models and numerical methods used must be considered when evaluating CFD outputs for the given application. Typically, the accuracy of numerical simulations, once they are shown to be independent of mesh and time step, is assessed by comparison with detailed experimental results including flow field data.

A number of turbulence models and numerical modelling techniques have been applied to model flows around bicycles and cyclists holding a static leg position. Table 3 presents the numerical work completed on flows around cyclists and the various modelling and validation techniques used. Defraeye et al. [27] compared a range of RANS steady-state simulations utilising various turbulence models and also transient large eddy simulations with experimental wind tunnel studies of a scale model of a cyclist. Of all the models tested, the strongest correlations with the wind tunnel data were obtained with the RANS Shear Stress Transport $k-\omega$ model. This model has also been used by others to model the flow around bicycle components [44]. Good comparisons with experiments were also reported with the standard $sk-\epsilon$ model utilising

low-Reynolds number modelling treatment of the viscosity-affected near-wall regions.

Griffith et al. [14] have found strong correlations with the experimentally obtained flow fields using a transient (Scale-Adaptive) SST simulation of various static leg positions around the pedal stroke. Although steady-state simulations modelled asymmetrical leg positions reasonably well, they did not accurately model the flow field when the cranks were close to a horizontal position. This was due to the limited ability of a steady-state numerical simulation to accurately model flows that exhibit significant time dependence, as observed around the more 'symmetrical' leg positions. In these phases of the crank cycle, time-averaged transient simulation results provided the best comparison with time-averaged velocity fields obtained from wind tunnel experiments. The improved accuracy came at a significant cost, but with the computing time required for the transient simulation compared the steady state increasing by up to a factor of 40.

3.5 Track and road testing

While wind tunnel testing and, more recently, CFD have taken over as the primary analysis techniques for studying cycling aerodynamics due largely to their accuracy, reproducibility, and the insight that they can provide into the basic mechanisms that create drag over a cyclist, field

testing methods have played and will continue to play a major role in the development of this field of research. It is very important that expected aerodynamic improvements within a wind tunnel are compared to the measured performance in the field, as ultimately performance in the field is the true metric of success for any aerodynamic optimisation. Finally, field testing methods, while prone to larger uncertainties, may be more readily performed if wind tunnels or high-end workstations for CFD analysis are not available.

With the introduction of on-bike power meters such as the Schoberer Rad Meßtechnik meter (SRM) in the mid-1990s, it became possible to directly measure the amount of power required to power a bike at a given speed. In preparation for the 1996 Olympics, the United States pursuit team underwent on-track pacing sessions, in order to investigate rider positions and equipment [45]. The bicycles were instrumented with power meters, from which average power data in each of the team pursuit positions 1–4 for each team member were analysed (corrected to a constant speed of 60 km/h). This investigation yielded relative quantitative results, and as the authors noted, it was strongly influenced by the cyclist's ability to execute even pacing and maintain a consistent draft (both laterally and fore-aft). Furthermore, while this procedure did ascertain the total resistive force on the cyclist (which was most relevant for the purpose of the US Olympic Team), it did not distinguish between aerodynamic drag and other

Table 3 Numerical simulations of the flow around various cycling-based applications

Study	Application	Simulation	Cell count, Δt	Position	Crank	Validation	Variation
[37]	Drafting	Steady, $sk - \epsilon$	12.0×10^6	U,D,TT	$0°$	Athlete-C_DA	0.7–10.5
[40]	Rider + vehicle	Steady, $sk - \epsilon$	27.9×10^6	TT	$0°$	1:4 model-C_DA	Other
[41]	Rider + vehicle	Steady, $sk - \epsilon$	34×10^6	TT	$0°$	1:4 model-C_DA	<3
[42]	Rider	Steady, $k - \epsilon$	4.6×10^6	U,D,TT	$0°$	Athlete-C_DA	7–13
		Transient, LES	4.3×10^{-4} s	U,D,TT	$0°$	Athlete-C_DA	3–13
[27]	Rider	Steady, $k - \epsilon, k - \omega$	7.7×10^6	U	$0°$	1:2 model-C_DA^*	−36 to 72
		Transient, LES	4.3×10^{-4} s	U	$0°$	1:2 model-C_DA^*	−6
[36]	Rider	Steady, $sk - \epsilon$	7.7×10^6	U,D,TT	$0°$	Athlete-C_DA	Other
[38]	Team pursuit	Steady, $sk - \epsilon$	21.2×10^6	TT	$0°$	Other	–
[43]	Rider + bicycle	Steady, $k - \epsilon, k - \omega$	17.9×10^6	D	$0°$	1:1 model-C_D^*	−12 to −7
		Transient, LES, DES	1×10^{-5} s	D	$0°$	1:1 model-C_D^*	−17 to −5
[35]	Wheels	Steady, SA	$6–11 \times 10^6$	–	–	Other	–
		Transient, DES	$6–11 \times 10^6$	–	–	Other	–
[14]	Rider + bicycle	Steady, SST	33×10^6	TT	$0°–180°$	1:1 model-C_DA	−13 to −17
		Transient, SAS	4×10^{-4} s	TT	$15°, 75°$	1:1 model-C_DA	−13 to −15

For brevity, the exact details of the simulations, such as the use of wall functions, standard/realisable models, or additional modelling techniques utilised, are notshown. Only the variation between numerical and experimental drag area/coefficients is shown for investigations in which theexperimentally obtained data were directly apart of the study in question. The superscript * symbol refers to when additionalcoefficients have been compared with the experimentally obtained values

sources of resistance such as wheel rolling and bearing resistance.

Debraux et al. [28] reviewed several field testing methods, targeted specifically at separating aerodynamic drag from rolling resistance. Several methods rely on measuring the deceleration of a free-wheeling cyclist at preset intervals and then fitting the data to a simple one-dimensional dynamic model of the motion (coast downs). A free-wheeling cyclist travelling in a straight line will be subject to aerodynamic drag and rolling friction 'F_{RR}' that will decelerate the cyclist. Additionally, some protocols prescribe that the test be performed while coasting uphill, meaning that a component of the gravitational force 'F_G' will directly oppose the motion. Therefore, the basic equations of motion can be written as

$$\text{ma} = F_D + F_{RR} + F_G = -\frac{\rho U^2 C_d A}{2} + mg_0(C_{rr} + \sin\theta), \tag{11}$$

where 'm' represents the mass of the cyclist–bike system, 'a' the cyclist's acceleration, 'U' their velocity, 'C_{rr}' the coefficient of rolling resistance, and '$g_0 \sin\theta$' is the gravitational acceleration due to an uphill slope at angle θ. As the drag of a cyclist varies considerably over the course of a pedal stroke [12, 15, 46], the most representative coast down tests require riders to spin their legs without applying power to effectively average the $C_d A$ over the pedal revolution cycle.

In addition to deceleration methods, the final noteworthy method is another curve fitting technique that uses power data directly from an on-bike power meter, known as the linear regression method. In this method, a rider aims to maintain constant power and speed over a flat course. The test is repeated at several different speeds (alternately, the power may be chosen as the independent parameter). At a constant speed on flat terrain, the total resistive force is simply the sum of the aerodynamic and rolling resistance. The measured power 'P_m' is then related to these forces by the following expression:

$$P_{m/v} = \frac{\rho C_d A}{2} U^2 + mg_0 C_{rr}. \tag{12}$$

By measuring the power at several fixed speeds, the values of $C_d A$ and C_{rr} can be extracted using linear regression, assuming that ρ is known from the local weather conditions. It should be noted that this method cannot be used without modification in a track due to the normal forces induced by the turns.

4 Optimising single-rider aerodynamics

Minimising aerodynamic resistance through rider position is one of the most effective ways to improve performance among well-trained athletes. Recent studies utilising modern

aerodynamic bicycle geometries suggest that the rider contributes $\approx 80\%$ to the total aerodynamic resistance acting on the bicycle–rider system [14]. As the rider contributes the largest proportion to the aerodynamic forces, optimising the aerodynamics of the body will likely see the largest gains in cycling performance. The greatest influence one can have on the aerodynamics of the rider is through the adjustment of cycling position. This was identified in an early wind tunnel study conducted by Kyle and Burke [3] which led them to propose a three-tier hierarchy for reducing cycling resistance: (1) the position of the rider, (2) the geometry of the bicycle (or more generally cycling equipment), and (3) the methods for minimising the rolling resistance and drive-train friction losses. Although the biomechanics and physiological efficiency of cycling are outside the scope of this review, when optimising cycling performance, the power output and fatigue characteristics of cyclists must also be weighed up against any apparent gains in the aerodynamic performance through adjustment to position [47–49]. Any changes to rider posture must also be considered along with current UCI rulings on legal rider positions.

4.1 Wind tunnel testing of rider position

The importance of position has prompted many wind tunnel investigations into the main positions used by elite cyclists, which are depicted in Fig. 8. Table 4 shows the reported drag area and drag coefficients from the wind tunnel testing of cyclists in various positions. Overall wind tunnel investigations are largely consistent in the relative ranking of these postures in terms of aerodynamic performance. The time-trial position has the lowest aerodynamic drag followed by the drops position and the upright break hoods and stem positions exhibiting the highest aerodynamic drag. Average wind tunnel data suggest that the reduction in drag between an upright sitting position with straight arms (such as the *stem* and *hoods positions*) and a *drops position* can be as much as 15–20%, and for the time-trial position as much as 30–35%. However, these are only average results and drag area and coefficient measurements for the time-trial position widely used today vary by as much as 40% between separate wind tunnel studies, and as much as 60% between wind tunnel studies and other indirect methods of determining drag [50].

There are a number of reasons why reported aerodynamic forces and coefficients vary significantly for each of the main positions between separate wind tunnel investigations. Differences in atmospheric conditions, drag measurement devices, wind tunnel type, blockage effects, Re effects, and freestream flow quality are all specific characteristics of wind tunnels and all affect aerodynamic force measurements [32]. Another source of variation between
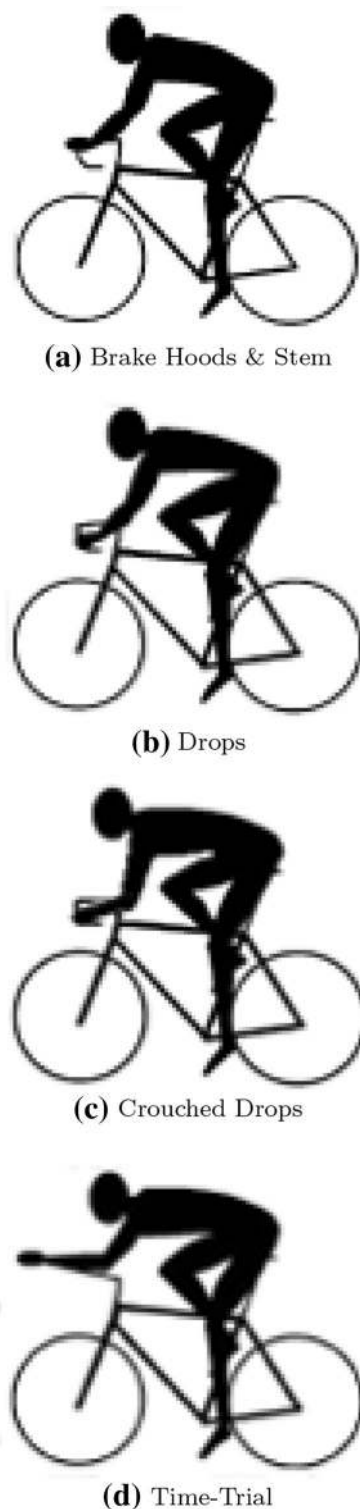
(a) Brake Hoods & Stem

(b) Drops

(c) Crouched Drops

(d) Time-Trial

Fig. 8 The traditional positions and the time-trial position. Reprinted from Gibertini and Grassi [8], p 32–33, with permission from Springer

wind tunnel investigations into rider position is differences in test methodologies and whether tests have been conducted with static or pedalling riders. The time-averaged

drag force is not necessarily well represented by a static cyclist and significant variations in aerodynamic drag between static and pedalling cyclists have been reported [51]. Current research suggests that the drag coefficient of a pedalling cyclist is ≈6% higher than that of a static cyclist holding a horizontal crank position [12]. Although it is difficult to make direct comparisons between different wind tunnel studies, which may not state the specifics of the testing environment and equipment used, the greatest contribution to the dissimilarities in the research is most likely due to rider aspects such as variation in rider position and anthropometric characteristics (rider size/shape).

Despite many wind tunnel investigations into the aerodynamics of cyclists, these have not been able to explain the large variation in aerodynamic drag that is observed between different rider geometries and subtle changes to position. As the drag force is sensitive to rider shape and position, it is difficult to identify specific rider attributes that contribute significantly to the large variations in aerodynamic drag that have been observed among cyclists for a given position. A study by Zdravkovich et al. [53] looked at the drag coefficient for two different athletes of similar height and mass, and a 1:2.5 scale model of a bicycle and rider in the brake hoods position, drops position, crouched drops position, and the time-trial position. Wind tunnel measurements showed that the brake hoods position had the highest drag coefficient followed by the drops and crouched drops position, with the time-trial position recording the lowest drag coefficient. However, there were large variations in the drag coefficient between each of the two athletes and the model for similar positions. This was most noticeable between the two athletes with the drag coefficient varying as much as 30% between them for a similar position. This led Zdravkovich to conclude that a single value of drag coefficient cannot be specified for any one position or cyclist, a result of the strong dependence of the drag coefficient on the size and shape of the rider.

Other studies by Gibertini and Grassi [8] have also looked at the effect that position can have on how streamlined a rider is. In contrast to findings by Zdravkovich et al. [53], wind tunnel tests of an experienced rider in the stem, brakes hoods, drops, and time-trial positions revealed that the most streamlined position for this rider (indicated by the drag coefficient) was not that of the time-trial position (0.792) but of the brakes hood position (0.760). This was despite the projected frontal surface area being 37% higher for the brakes hood position. Drag area measurements for the brakes hood position however were 30% higher than those for the time-trial position, indicating that it was more important to reduce the frontal area for this particular rider.

Although minimising frontal area is clearly important, as demonstrated by the widespread use of the time-trial

Table 4 Reported drag coefficient and drag area measurements from wind tunnel testing of cyclist position

Studies	Measurement	Upright	Dropped	Time-trial	Crank	Velocity (m/s)	Blockage
[52]	C_D	1.140–0.912	–	–	Static	4.8–21.0	–
[53]	C_D	0.750–0.600	0.690–0.520	0.600–0.490	Static	8.2	12.4–16.2%[!]
[54]	C_D	–	–	0.650	Static	13.9	–
[8]	C_D	0.824–0.760	0.814	0.792	Dynamic	13.9	$\approx 2\%$[!]
[51]	C_D	1.33	–	0.99–0.96	Dynamic	15	<5.5%[!]
[49]	C_D	–	–	0.864–0.803	Dynamic	11.1	> 10%[*]
[55]	C_D	0.69	0.71–0.66	–	Dynamic	12.5	<9%[*]
[56]	$C_D A$ (m^2)	–	0.28	–	Dynamic	1.5–18.5	–
[3]	$C_D A$ (m^2)	0.32	0.26	–	Static	8.9–15.6	8%[!]
[2]	$C_D A$ (m^2)	–	–	0.269	Dynamic	13.4	8%[!]
[54]	$C_D A$ (m^2)	–	–	0.244	Static	13.9	–
[57]	$C_D A$ (m^2)	0.358	0.307	0.269–0.240	Static	12.8	–
[51]	$C_D A$ (m^2)	–	–	0.260	Static	15	<5.5%[!]
[51]	$C_D A$ (m^2)	0.521–0.428	–	0.293–0.341	Dynamic	15	<5.5%[!]
[8]	$C_D A$ (m^2)	0.318–0.282	0.289–0.275	0.235–0.223	Dynamic	13.9	$\approx 2\%$[!]
[49]	$C_D A$ (m^2)	–	–	0.296–0.226	Dynamic	11.1	> 10%[*]
[42]	$C_D A$ (m^2)	0.270	0.243	0.211	Dtatic	10–20	<6%[!]
[55]	$C_D A$ (m^2)	0.343	0.332–0.295	–	Dynamic	12.5	<9%[*]
[58]	$C_D A$ (m^2)	–	–	0.251–0.214	Dynamic	18	<5%[*]

The majority of 'static'-based wind tunnel studies appear to be performed with the legs approximately holding a horizontal crank position, and the superscript $*$ and ! symbols refer to studies that were conducted in an open-jet or a closed test section, respectively

position, frontal area is not always the dominant factor when comparing the aerodynamic drag of different riders in similar positions. It is a common misconception that the most aerodynamic riders and positions are the ones that also exhibit the smallest possible frontal area. As the drag coefficient will vary with frontal area (due to change in rider position), minimising one will not necessarily result in a minimum in the drag area. The degree to which the drag coefficient can affect the performance of a cyclist is highlighted in two separate studies reported on by Bassett et al. [59]. Both investigations involved measurements of aerodynamic drag and frontal surface area of cyclists in a wind tunnel at 13.3 m/s. The findings demonstrated a weak correlation between measured aerodynamic drag and frontal area, of which the frontal area only accounted for $\approx 50\%$ of the variation in drag between the different athletes and their positions.

There have been many 'rules of thumb' developed regarding optimal positioning of a cyclist's arms, legs, torso, and head [57, 60–62]. Even relatively minor alterations to one's time-trial position can have a large effect on aerodynamic drag. Broker [61] and Kyle [62] note that rider positions that result in a flat back, a low tucked head and forearms positioned parallel to the bicycle frame generally have low aerodynamic drag. Wind tunnel

investigations into a wide range of modifications to standard road cycling positions by Barry et al. [55] showed that that lowering the head and torso and bringing the arms inside the silhouette of the hips reduced the aerodynamic drag. Positions that resulted in reductions in aerodynamic drag were also related to a lower velocity deficit and turbulence levels in the wake. Studies by García-López et al. [51] and Underwood et al. [49] have shown that reducing the torso angle generally results in a reduction in aerodynamic drag. However, these studies also showed that minimising torso angle did not always lead to the lowest aerodynamic drag readings.

The effectiveness of rider equipment, such as bicycles and helmets, is also dependent on the position and type of rider [51, 63–65]. For these reasons, the most effective method to optimise a cyclist's aerodynamic performance to date has largely been through a trial-and-error approach to force measurements in a wind tunnel. The position of the cyclist, usually defined by the set-up of the bicycle (handle bar and seat positions), and cycling equipment are continually refined until rider position and equipment configurations are identified which result in a lower drag compared to baseline force measurements. Current studies into cycling position have primarily focused on the variation in aerodynamic drag with posture as this directly

relates to cycling performance. The direct link between the measured variations in the aerodynamic drag force and the flow field around different cyclist geometries is currently not well understood.

4.2 Cycling equipment—design for aerodynamic performance

Despite tight UCI regulations on streamlining equipment, aerodynamics is a major design criterion of elite-level cycling equipment. The footprints of aerodynamic styling are embedded all over the designs of bicycle frames, wheels, helmets, and skin suits. In addition to reducing weight, improving power transmission, and bicycle stability and bicycle control, enhanced aerodynamics offers equipment manufacturers a direct link to increasing rider speed and improving cycling performance. Savings in aerodynamic drag due to superior equipment that does not involve altering rider position are often referred to as 'free energy' as performance gains do not require lengthy training programmes or changes to cycling technique. Although aerodynamic styling targeting drag reduction is often the most visual and recognised aspect of streamlined equipment design, aerodynamics is also critical to other equipment design criteria. These include maintaining stability and control during windy on-road conditions and improving athlete cooling and heat transfer, which is important for endurance events.

To effectively improve aerodynamic performance, cycling equipment must be designed for the local flow field in which it is operating. The true measure of the aerodynamic performance of equipment is not how well it performs in isolation, but how well it is integrated with the complete bicycle–rider flow field. Much of the early work on improving the aerodynamic performance of cycling equipment was done separately from the rider. There are many examples where measured aerodynamic savings resulting from new equipment designs have been significantly reduced or are non-existent when the rider is added to the system [61]. Clearly, the dominant impact of the rider on the global flow field and flow interactions occurring between equipment and rider must be considered to effectively optimise equipment and rider aerodynamics. Performance parameters resulting from studies and equipment designed in isolation of a complete bicycle/rider system should be treated with caution.

The other main consideration when optimising the aerodynamic performance of equipment is the environmental conditions that will likely be encountered on the road or track. Road cyclists compete within a turbulent atmospheric boundary layer that exhibits gusty wind profiles that are rarely aligned with the direction of travel. Cross-winds result in flow asymmetries being generated around the bicycle and rider, as demonstrated in Fig. 9a, which not only affects the magnitude of the aerodynamic drag force but also generates additional side forces, rolling, and yaw moments. These forces and moments can result in a cyclist being unable to maintain control of their bicycle. Typically, aerodynamic styling to minimise drag is at odds with reducing aerodynamic side loads, rolling, and yaw moments and is why aerodynamic design to minimise these forces and moments is particularly important at the elite level. Gusty cross-wind conditions have resulted in a number of elite cyclists losing control during windy road racing events [67, 68]. Although not as severe as on the road, cyclists in a velodrome also experience asymmetric flow conditions when in close proximity to another athlete or while negotiating corners of the track. Recently, this has led to the development of bicycle frames and wheels by equipment manufacturers specifically for asymmetric flow conditions experienced while circling the velodrome [69].

Atmospheric and freestream turbulence characteristics are another critical aspect of environmental flow field conditions that can have a significant impact on aerodynamics performance. Effective design for turbulent 'on-road and on-track' conditions is an area that is not well understood for complex three-dimensional geometries, even in much more advanced fields of bluff body aerodynamics such as road vehicles. In the relatively controlled environment of the velodrome, cyclists are still embedded in a turbulent flow field resulting from wind currents generated by natural or forced convection and also the decaying remnants of turbulent eddies left in the wakes of team members and other competitors. The exact mechanisms by which freestream turbulence influences flows around bluff body aerodynamics are complex and often difficult to predict. For simple geometries, the effects of freestream turbulence are known to induce transition to turbulent boundary layers sooner (effectively reducing the critical Reynolds number) and increase mixing and spreading rate characteristics of turbulent wakes, both of which can have significant implications on the magnitude of aerodynamic forces. A simplified schematic of these processes from Bearman and Morel [66] is depicted in Fig. 9b. Given that current standard practice is to set rider position and optimise equipment designs in low-speed, low-turbulence wind tunnels, that in many scenarios will not be representative of track conditions, techniques and methods for tailoring equipment aerodynamic performance for turbulent flow fields are currently not well developed.

4.2.1 Bicycle frames

Surprisingly, little has been published in peer-reviewed articles that focus specifically on the aerodynamics of bicycle frames. The most notable exceptions are that of
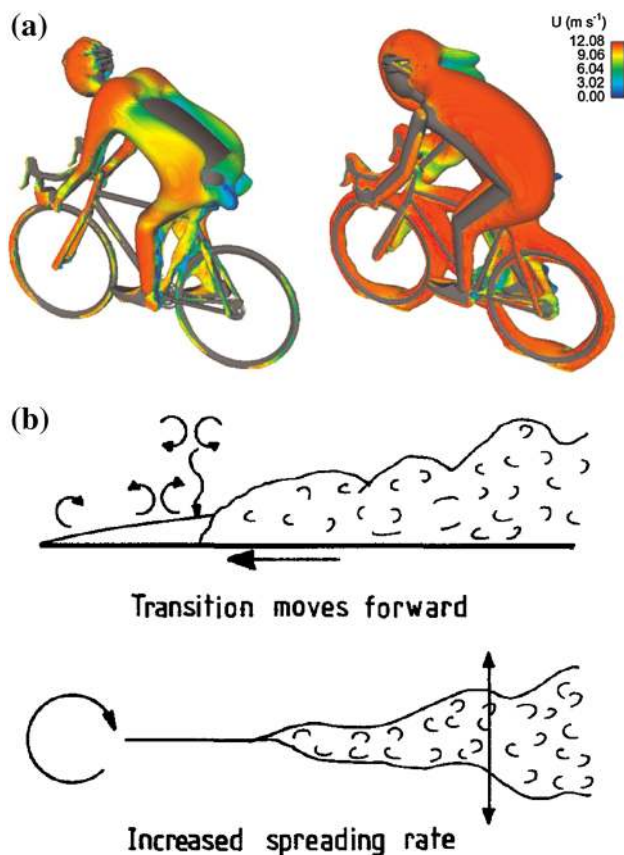
Fig. 9 a CFD simulations by Fintelman et al. [43] comparing isosurfaces of the pressure coefficient coloured by velocity for 0 and 60° flow yaw angles. It is evident that cross-wind conditions will induce asymmetries in the location at which flow stagnation and separation will occur leading to asymmetric pressure and flow field distributions around the bicycle and rider. Reprinted from Fintelman et al. [43], p 37, ©2015, with permission from Elsevier. **b** Generalised depiction of the influence freestream turbulence can have on transition and mixing from Bearman and Morel [66]. Reprinted from Bearman and Morel [66], p 103, ©1984, with permission from Elsevier

Zdravkovich [70] and Parker et al. [65] who performed early investigations into methods to improve bicycle frame aerodynamics. In an attempt to streamline a traditional round tube frame, Zdravkovich [70] looked at the effectiveness of adding splitter plates. Aerodynamic savings were limited using splitter plates and it was concluded that a much more practical method of reducing drag on the frame was streamlining the tubing (using tear-dropped or airfoil cross-sections). Parker et al. [65] showed that the aerodynamics of the frame could be improved by adding a faring to close the main triangle of an open frame, which is now illegal under current UCI regulations. Parker et al. [65] also highlighted the importance of rider position on frame aerodynamics. They showed the potential to improve rider aerodynamics through decreasing the width of the bottom bracket and reducing the gap between the legs and both an open and a closed frame geometry. Apart from

these and other minor studies, the vast majority of bicycle frame development has occurred within industry and the exact design details and flow physics of their frames are not easily assessable. Despite this, we can see the impact that aerodynamics has had on the design of modern bicycles.

The main driving forces behind bicycle design for elite athletes over the past 50 years have been primarily a result of a greater understanding of the importance of aerodynamics on cycling performance, advances in materials, and composite layup techniques and regulations on bicycle design set by the UCI. These influencing forces on bicycle design are evident in Fig. 10 which compares bicycles used by Olympic gold medallists in the individual time-trial (now part of the Omnium) over the past 35 years to a traditional round tube frame that was typical prior to the 1980s (in this case the bicycle used by Eddy Merckx in his successful 1972 world hour record attempt).

One of the first bicycles designed with aerodynamics in mind was a result of the 'Elite Athlete Project' started by the US Olympic committee. To improve its chances at cycling success at the 1984 Olympics, the US, who had not won a medal in cycling in over 70 years, developed track cycles for the US Olympic track cycling team using a low-speed wind tunnel test programme with a focus on minimising aerodynamic wind resistance. The bicycles, known as 'funny bikes', employed a number of features to reduce aerodynamics resistance. These included streamlined aluminium alloy tubing to construct the frames, cow horn handlebars, and frame geometry to improve rider position, and disc and flat spoke wheels. The bikes were also designed with the use of smaller than standard wheels at the time. Smaller wheels were said to improve the drafting effect in team events, as riders could sit closer together in a pace-line. For individual events, a smaller front wheel in combination with a standard size rear wheel (now illegal under current UCI rules) was said to improve the aerodynamics of rider position.

Towards the end of the 1980s, advances in the use of composites to construct light-weight frames led to the development of several exotic bikes used in competition that departed substantially from the traditional double diamond frame. Several companies, Zipp and Lotus being two notable examples, developed what they considered "super bikes" which consisted of monocoque frames. These bikes capitalised on the moldability of carbon fibre layups to create stiff structures that served not only as structural members but also as aerodynamic fairings, and often did away with extraneous tubing such as the top or down tube, and occasionally one or two of the stays in the rear triangle of the frame. When tested in isolation of a rider, these bikes proved to produce substantially less drag than their more conventional counterparts. In the early 2000s, the UCI mandated a return to more conventional
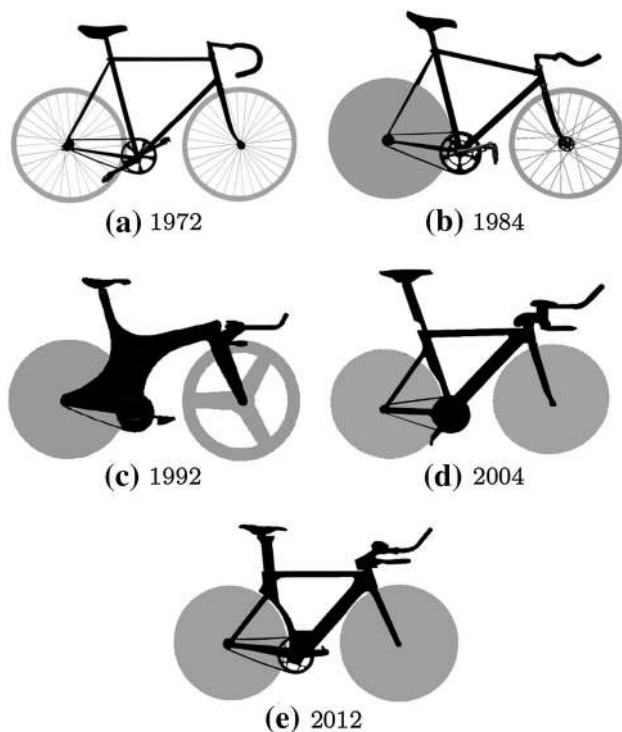
Fig. 10 Bicycles used by Olympic gold medallist competing in the individual pursuit compared with a traditional round tube frame and double diamond frame geometry common until the early 80s in elite cycling

geometries for competition, effectively ending much of the work that was being done on the monocoque super bikes. The UCI added a further restriction in 2009, known as the "3:1 rule", restricting the cross-sections of the tubes that make up the frame to a length-to-width ratio of 3:1 [71, 72].

Although reducing wind resistance on the frame is important, it will always be limited as the majority of the wind resistance acts on the rider. Bicycles that have resulted in the largest gains in elite cycling performance have been achieved through designs that target the aerodynamics of rider position. Today, time-trial bars, which act to both reduce frontal area and streamline the rider, are a must have for any serious time-trial competitor. When they first started appearing on the scene in the late 80s however this was not the case. In the final stage of the 1989 Tour de France, a 25-km time-trial to Paris, Greg LeMond, who was 50 s behind the race leader Laurent Fignon going into the final stage, rode with time-trial bars and an aero-helmet, whereas Fignon rode with a wide dropped position and no helmet. Lemond, who was thought to have little to no chance of claiming victory, ended up winning the 1989 Tour by just 8 s over Fignon who conceded 58 s to LeMond on the final stage. To this day, this is the smallest winning margin in the history of the Tour de France. It is widely accepted that the superior position and aerodynamics of

LeMond had the most significant impact on his 1989 victory. Other classic innovations in bicycle design, with a focus on improving rider position, can be seen in bicycles developed by Graeme Obree for the world hour record (see Sect. 1.1).

Compared to bicycle frame development of the early 90s, restrictions imposed by the UCI after 1996 have meant that aerodynamic improvements today are achieved through relatively minor modifications to a standard frame with aerodynamic tubing. Modern frames adhering to the "3:1 rule" are designed using both wind tunnel and CFD techniques with a focus on improving the aerodynamic interactions between the frame, front and rear wheels, and the rider. Currently, the major area for development in bicycle technology has occurred in triathlon. Relaxed rules on frame geometry, rider position, and the addition of food storage, hydration, and electric gear shifting systems gives bicycle designers much more room to move to improve bicycle aerodynamics. Today, these low-profile bikes incorporate internal cabling, concealed brakes, frame cut-outs to hold moulded hydration systems, and electric battery packs integrated into the frame design all in an attempt to minimise wind resistance and set them apart from their competitors.

4.2.2 Wheels

Wheels make up a major component of the bicycle and have been the subject of a substantial amount of analysis into cycling aerodynamic performance. The magnitude of the aerodynamic forces and moments acting on wheels is highly variable, particularly when we consider the large range of shapes and designs (spoke wheels to deep rim wheels to disc wheels) and the environmental conditions in which they operate. The aerodynamic properties of spoked wheels received a substantial amount of study beginning in the early 20th century on aircraft with fixed landing gear, and later for their application on motorcycles [70]. In contrast to those earlier studies, however, the form factor of the bicycle wheel, as classified by the ratio of the wheel diameter to the tyre diameter, is much higher, owing to their small size and relatively high inflation pressures.

Over the last 15 years, a number of studies have looked at cycling wheels under yawed flow conditions. These studies have looked at spoked wheels with various rim profiles, as well as unconventional spoked wheels and disc wheels. A substantial body of work on the specifics of wheels, however, remains either proprietary or has been published as unreviewed white papers or articles. Nonetheless, there have been a number of studies conducted both in wind tunnels and, more recently, using CFD.

Tew and Sayers [73] performed a wind tunnel study, examining six different wheels: a conventional spoked

wheel, a low-spoke count wheel, a bladed spoke wheel, two wheels with a small number (three or four) of structural bladed carbon spokes, and a disc wheel, which are depicted in Fig. 11. Drag and side force coefficients were measured for yaw angles up to 30°. With the exception of the conventional spoked wheel, all of the remaining spoked wheels featured deep rim profiles, nominally intended to reduce the wake behind the rim and, thus, the drag of the wheel. For non-yawed conditions, the disc showed a 70% reduction in the drag coefficient over the conventional wheel, while spoked, deep section wheels were well clustered about 60% below the conventional wheel. A critical characteristic of the deep section wheels that the authors observed was a nearly flat drag coefficient across the yaw angles and wind speeds. The disc, however, showed a sudden increase in the drag coefficient at intermediate yaw angles, particularly at low speeds. The critical angle increases with speed, and the sudden nature of this rise suggests a boundary layer separation effect.

In recent years, a significant amount of work has been done using CFD. Godo et al., in particular, have produced some of the most extensive CFD analyses of wheels [34, 35] and the interaction between the front wheel, the fork, and the down tube [74]. Going beyond the capabilities of wind tunnel analysis, Godo et al. [34, 35] were able to resolve the contributions of the various components of a wheel—hub, spokes, and rim—to the overall drag of the system. These studies simulated the flow around the wheel in isolation of the bicycle–rider system. Steady-state simulations were run from 0° to 20° yaw. Transient simulations were also performed that simulated the rotation of the wheels at an equivalent ground speed of 20 and 30 mph.

Both of these studies by Godo et al. compared their simulation data to various published wind tunnel results for the various wheels, taking data from both peer-reviewed sources and equipment manufacturers' white papers. The authors noted the similar discrepancies to those that have been noted above, with the drag coefficient at zero yaw (theoretically the cleanest and simplest case) varying by a factor of two across many of the different experimental studies. This highlights the magnitude of uncertainty associated with aerodynamic forces and moments acting on wheels as a result of variability in test fixtures, measurement apparatuses, and wind tunnel conditions. As such, while the results by Godo et al. followed qualitatively similar trends as much of the experimental data and generally fell within the quantitative range of the data, a direct comparison is not really possible.

For the deep profile spoked wheels (the Zipp 404, 808, and 1080), the CFD data showed very good agreement in the trends, and the CFD analysis showed that all three wheels had a minimum drag coefficient occurring at 10° for all three wheels, whereas the drag coefficient of the conventional spoked wheel remained flat up through 14° before beginning a slow rise. Curiously, these results show that the three deep profile wheels only perform substantially better than the conventional wheel over a small range of yaw angles centred around 10°, although as the rim depth increases, that range increases. For the disc wheel, the drag dropped over the entire range of yaw angles; however, the study was unable to replicate a proprietary result by Zipp, which showed that the drag coefficient dropped below zero over a small range, supposedly producing a net propulsive force. By resolving the pressure and viscous contributions to drag separately, however, they did show that the pressure force on the disc was negative (propulsive) at 8° and above 14°, but was overwhelmed by the viscous (friction) component of the drag. This suggests that the "sail" effect is real, but that the total drag on the wheel is sensitive to the boundary layer properties (and consequently the freestream turbulence).

A time-resolved analysis of the wheels showed the formation of several recirculation zones at the upper and lower sections of the wheel. These recirculation zones were seen to be the largest on the disc and trispoke compared to the conventionally spoked wheels. Mechanistically, it seems clear that the formation of these flow structures and their periodic disruption by the spokes play a critical role in the production of drag; however, the analyses have not yet gone into sufficient depth to understand their role. The studies did explore other aerodynamic forces and moments experienced by the wheels, including side force, vertical force, and turning moments, were also examined; however, those are omitted here, as their role in performance is less clear.

4.2.3 Helmets

The location of a rider's head relative to the flow and its size relative to the rest of the system mean that the choice of helmet can have a significant effect on the net drag force that the rider must overcome. As the effects of aerodynamic drag on performance have become more widely acknowledged, helmets initially designed to meet the safety standards set forth in various jurisdictions while providing substantial ventilation for thermal comfort have given rise to specially designed time-trial helmets. Modern time-trial helmets are designed for speed over comfort and, more recently, has led to the development of hybrid helmets that attempt to reduce drag without compromising ventilation and mobility. This focus on helmets arises from the relative magnitude that a rider's head and helmet have on the overall drag, noting that some studies have shown that the difference between well-performing helmets and poorly performing helmets can be greater than the difference between fast and slow wheels [75].

Fig. 11 Various commercially available wheel designs tested for aerodynamic properties by Tew and Sayers [73], including **a** traditional 36-spoke, **b** 16-spoke, **c** 12-spoke, **d** quad-blade-spoke, **e** tri-blade-spoke, and **f** disc wheel designs. Reprinted from Tew and Sayers [73], p 213, ©1999, with permission from Elsevier
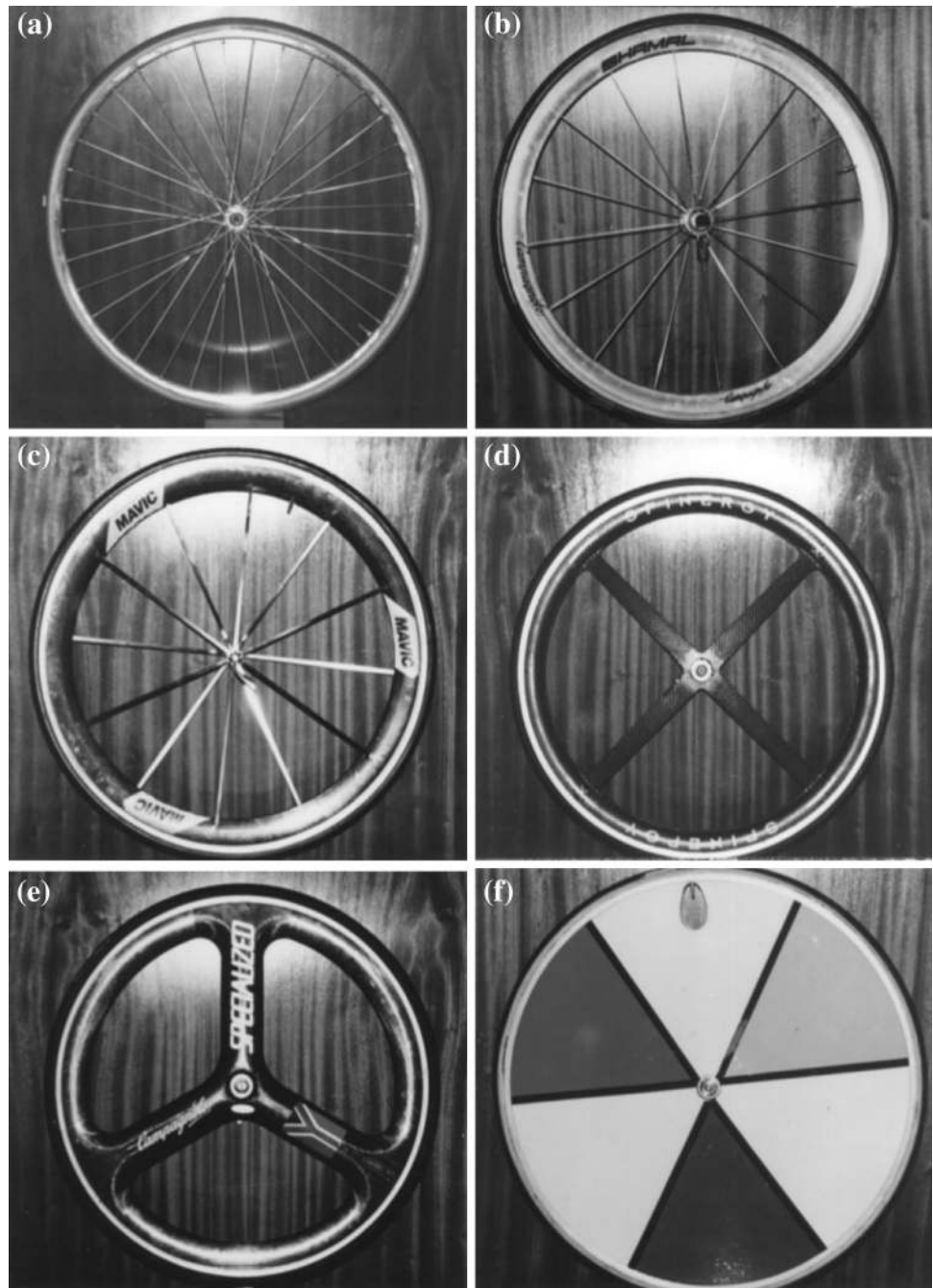
Long-tailed helmets, which cover the rider's head in an elongated fairing, have been the subject of several studies that have compared different helmets, as well as the manner in which they are worn as well as their context (geometry of the rider's head and back). Blair and Sidelko [63] conducted an experimental investigation of 14 time-trial helmets (accounting for helmets that came with a detachable visor) using a mannequin that represented the upper body of a cyclist at several different yaw angles [75]. In addition, the helmets were mounted in three positions, based on the inclination of the leading edge. The results showed a global reduction in drag of up to 10% for well-performing helmets compared to poorly performing helmets. Extremely high inclination angles resulted in high drag across the board; however, no mechanistic correlation between helmet design and performance was identified.

Chabroux et al. [64] further showed that there is a strong interaction between the posture of the rider (comparing a more upright road posture with a low time-trial posture)

and the drag force on the helmet. The study further showed that while a visor has a statistically significant effect, reducing the drag of the helmet, forward-facing vents do not tend to result in a drag penalty. Brownlie et al. [76], however, showed several cases in which the visor (or sunglasses) resulted in a slight increase in drag. Furthermore, this study showed that while, in general, a time-trial helmet has superior aerodynamics to a more conventional helmet, a time-trial helmet also produces less drag than a bare mannequin head. (With the absence of rough features and the like, a mannequin's head can be reasonably assumed to have a lower drag coefficient than an actual human head.)

Chabroux et al. [25] conducted a more detailed wind tunnel investigation using particle image velocimetry to investigate the wake structure behind three long-tailed time-trial helmets. The study experimentally showed the time-averaged velocity deficit behind these three helmets (all of which produced similar total drag); however, in the absence of a comparison to other helmets with substantially different characteristics, the authors were not able to present a mechanistic story of the drag characteristics.

The particular geometry of any particular helmet, as well as the geometry of the riders head and upper back, limits the ability to make generalisations about helmet design. While streamlined shapes are a clear advantage, small geometric effects, as well as visors, can positively or negatively influence the drag force on the helmet, depending on the rider's posture and shape. Careful placement of vents allows for some measure of cooling in time-trial helmets without significantly compromising their performance.

4.2.4 Skin suits

Textured fabrics have been used to improve the aerodynamic performance of many high-velocity sporting disciplines, most notably skiing, speed skating, and cycling. The fundamental flow mechanism responsible for aerodynamic performance gains using textured skin suits is the delay or movement of the separation point towards the back of the body. This effectively reduces the size of the wake leading to increases in wake pressures and reductions in the pressure drag component of the aerodynamic resistance.

In one of the first detailed investigations into skin suit aerodynamics and design, Brownlie et al. [26, 79] demonstrated the potential to improve cycling performance using a range of textured fabrics to treat specific areas of the body. The relative texture of fabrics is dependent on a number of parameters, such as yarn type and material, stitch pattern and density, thickness, cover factor, porosity, seam positioning, coatings, and fabric tension. All of these variables have been shown to be important when considering the aerodynamic performance of skin suits [80–83]. Using a range of textured fabrics (> 200), Brownlie et al. [26] performed wind tunnel experiments with cylinders, full-scale leg models, and pedalling athletes that revealed a number of aspects of skin suit design critical to aerodynamic performance. These include the following:

– The arms and legs exhibit transitional type behaviour for Re relevant to cycling.
– The motion of the legs throughout the pedal stroke combined with turbulence generated from upstream components of the bicycle and body reduce the effectiveness of textured fabrics to induce drag crisis on any part of the legs.
– In areas of attached flow, smooth fabrics should be used to target reducing skin friction.
– In areas of completely separated flow, such as the lower back, surface texture has a negligible effect on aerodynamic drag and any appropriate fabric may be utilised.
– Reductions in aerodynamic resistance can be accomplished through tight fitting apparel with few wrinkles and aligning seams with the airflow.

Using these points to guide fabric selection, wind tunnel testing with a pedalling cyclist holding a time-trial position showed that aerodynamic drag could be reduced by ≈4% using up to five fabrics to construct skin suits, compared to traditional suits not optimised for aerodynamic performance that typically used 1–2 different fabrics.

Critical to understanding the aerodynamic performance of skin suits is the process by which turbulence can be induced at lower Reynolds numbers. As the human body has components that resemble cylindrical cross-sections, modern skin suit development has its foundations deeply rooted in early work into the laminar–turbulent transition process of flows around, and the aerodynamic drag acting on, circular cylinders. It is noted in Sect. 2 that a turbulent boundary layer is less susceptible to flow separation over curved surfaces. Figure 12a reproduces results from Achenbach [77] who investigated the influence of the surface texture of circular cylinders in a pure cross flow on aerodynamic drag as a function of Re (where the cylinder diameter is the characteristic length scale). Achenbach's findings show that not only is the drag coefficient a function of the Re number but also the surface texture. With increasing surface roughness, defined by the roughness parameter k (ratio of the roughness height to the width of the body), the minimum drag coefficient $C_{D,min}$ or the critical point at which drag crisis is said to have occurred is shifted towards lower critical Reynolds numbers Re_c. One also notes that with increasing surface roughness the $C_{D,min}$ increases and that for $Re > Re_c$ the drag coefficient is higher for cylinders treated with a rougher surface finish.

isea INTERNATIONAL SPORTS ENGINEERING ASSOCIATION

As with cylindrical geometries, the aerodynamic drag acting on body components (particularly the arms and legs) also displays similar dependence on Re and surface texture. When optimising skin suit design, the choice of fabric will depend on the size of the athlete wearing the suit, cycling speed, air properties, and UCI regulations governing allowable fabrics. Modelling the body as a composite of simple geometries in isolation of one another in a pure cross flow has a number of limitations when attempting to minimise aerodynamic drag. This simplification does not take into account flow interactions between limbs and body parts and the influence the motion of the legs has on the flow field around the body.

In addition to this, the relative orientation of limbs, the wind angle, and freestream turbulence levels have all been shown to be the relevant factors when reducing aerodynamic drag [84, 85]. The influence of freestream turbulence intensity on the critical Re on two-dimensional cylinders is shown in Fig. 12b, from the work of Fage and Warsap [78]. One finds that for increasing freestream turbulence intensity the transition process which leads to drag crisis occurs at lower Re_c. (Note: Intensity is only one characteristic of turbulence that is of importance to bluff body flows. The geometric characteristics and relevant length scales of turbulence are also important to transition and mixing processes.) The defining characteristics of turbulence experienced on the road and track are currently not well understood. As skin suit aerodynamics is sensitive to the wind environment, the size, position, and shape of the rider, there is no one skin suit that will have texture optimised for all cycling conditions, athletes, and cycling positions.

5 Multi-rider aerodynamics and drafting

The ability of the riders to shelter themselves in the wake of others (known as drafting), and thereby reduce their own drag, is one of the defining aspects of most bicycle racing (with the exception of individual timed events such as time-trials and individual pursuits). The addition of other riders, however, has received little prior attention due to the complexity of the problem, sensitivity of the results, and difficulty in carrying out experiments and computations. In other fields of bluff body aerodynamics ranging from simplified 2D cylinders, surface-mounted cubes, and more complex bluff body geometries such as racing cars, interaction effects between flows around multiple bodies are known to influence the aerodynamic force on both trailing and upwind bodies [86–92]. Over the past decade, advances in computing power and experimental techniques have opened up a line of enquiry into drafting effects in cycling, and in particular the team
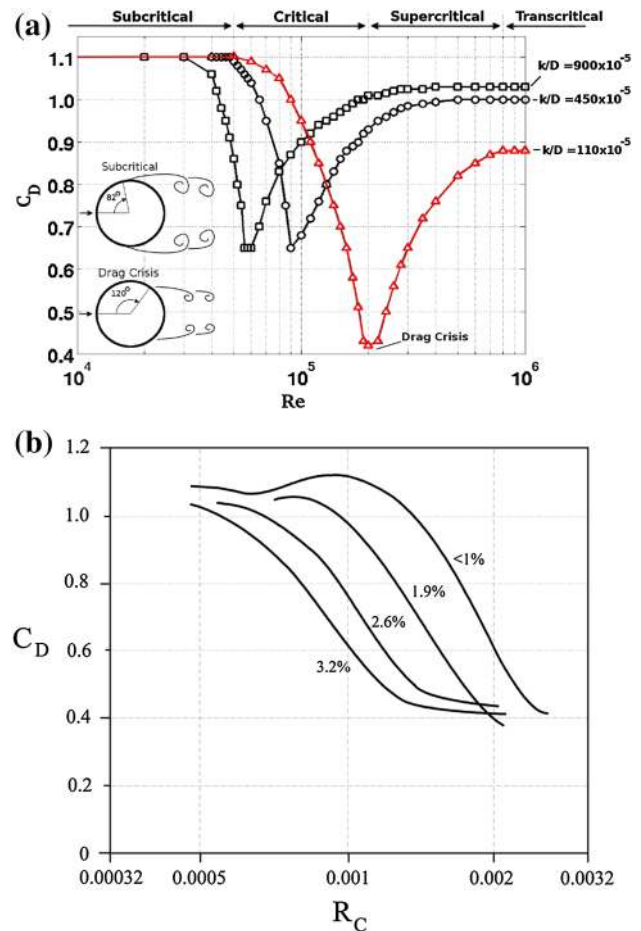

Fig. 12 a The drag coefficient of 2D circular cylinder of varying surface texture as a function of Re, reproduced from Achenbach [77]. The variation in C_D is related to changes in the flow regime around cylinders. The main flow regimes are labelled for the smoothest cylinder which is highlighted in *red*. Schematics demonstrate the relative difference in the wake width between a subcritical regime and the point at which drag crisis is said to have occurred. The actual flow topology of each regime is much richer than what has been depicted here. A summary of the various flow regimes and a more detailed description of the nature of the flow around cylinders for each regime can be found in Tropea et al. [6]. **b** Results reproduced from Fage and Warsap [78], who conducted some of the earliest studies into the influence of freestream turbulence on the drag coefficient and critical Re of 2D circular cylinders (colour figure online)

pursuit has provided the motivation to study multi-rider aerodynamics.

In the team pursuit, two teams of four riders compete by attempting to cover 4 km on the track in the fastest possible time. Team time-trials on the road are run in a similar configuration, often with up to nine riders on a team competing to complete a course in the fastest time. As both of these events are cooperative, the riders seek to both minimise their own drag and provide shelter to the other riders on the team. This is demonstrated in Fig. 13 which shows a wind tunnel smoke flow visualisation of a member

of a team pursuit team drafting in the wake of the lead rider. Studies focusing on these cooperative race schemes have sought to primarily answer four questions: how the aerodynamic drag force varies as a function of spacing from the lead rider, how much drag reduction do the multiple trailing riders experience, does the lead rider also experience a drag reduction, and what are the sensitivities of these results?

Studies addressing the influence of drafting distance on the aerodynamics drag of a single trailing rider are summarised in Fig. 14a. For a trailing cyclist positioned immediately behind the leader, drag reduction has been reported in the range of 15–50% and reduces to 10–30% as the gap extends to approximately a bike length. All findings show a relatively linear increase in C_DA of the trailing rider as the drafting gap is extended until the point at which the drag approaches the isolated rider value. This type of behaviour has previously been observed with other drafting bluff bodies such as racing cars [90]. Perhaps surprisingly recent investigations by Barry et al. [93] show that the wake of a trailing cyclists remains largely unchanged compared to the wake of an isolated rider. This is despite significant differences in upstream flow conditions that exist for isolated and trailing riders and highlights the robustness of the formation of the large-scale wake vortices.

It can be observed from Fig. 14a that although similar trends exist, large variations in the magnitude of the aerodynamic savings due to drafting are evident between the studies. In addition to the variability resulting from the different analysis techniques that have been utilised (previously discussed in Sect. 3), current literature suggests a number of reasons for these variations. The main contributing factors accounting for these variations are differences in the relative size, shape, and position between lead and drafting athletes and drafting skill (ability to maintain drafting gap and hold in-line position).

Kyle [94] was one of the first to establish a relationship between aerodynamic drag and in-line drafting distance using the coast down method. Tests were performed with a number of athletes over a 200-m coast down track which resulted in the relationship reproduced in Fig. 14a. Although no quantitative analysis of the variability of the coast down test was provided, it was noted that large variation in the data was present. This was likely due to the inability of the drafting riders to maintain a constant separation distance and axial alignment with the lead rider, an inherent issue with this sort of test technique. As drafting riders experience lower resistive forces than the lead rider, they will tend to decelerate at a lower rate. Despite the uncertainties associated with the coast down method to investigate drafting effects, the findings of Kyle [94] agree reasonably well with much more recent studies

conducted in the controlled environment of a wind tunnel [95].

Edwards and Byrnes [96] attempted to address how individual rider characteristics influence the drafting effect. The study found that not only is the drag area of the leader of critical importance, with a greater drag area (for the lead cyclist) corresponding to a greater drafting effect, but there appeared to be some interaction between the particular lead and trailing cyclists. The authors were unable to strongly correlate this interaction with anthropometric measurements of either the lead or drafting rider and postulated that, beyond drag area, drafting skill was the most probably one of the dominant factors determining the magnitude of the drafting effect.

In an effort to remove drafting skill from the equation, both Zdravkovich et al. [53] and Barry et al. [95] investigated the influence of drafting on aerodynamic forces in controlled wind tunnel experiments (see Fig. 14). Both studies note the importance of the drafting effect on the shape, size, and position of the riders. Despite differences in rider position between studies, the findings of Zdravkovich et al. [53] show a much more rapid decay of the drafting effect with separation distance compared to Barry et al. [95] and other relationships established in literature. It is evident that the findings of Zdravkovich would have been significantly influenced by wind tunnel blockage effects (>15%) due to the small closed wind tunnel test section in which experiments were performed. It is not reported whether these findings considered the close proximity of the wind tunnel walls to the test subjects.

In addition to characterising drag savings of in-line riders, both of these investigations also studied lateral offset positions of the trailing rider. Although the magnitudes differ substantially, both studies show a relative decrease in aerodynamic drag savings of the order of 30–10% for a 0.2 m lateral offset as axial spacing increases from ≈0 to 1 m. For overtaking manoeuvres, or more generally when riders are positioned alongside one another, Barry et al.'s [95] quasi-static results also showed that the relationship between aerodynamic drag and rider position is more complex compared to when the trailing rider is positioned aft of a leader's rear wheel. As a result of interference effects between riders, at certain positions throughout a relatively close overtaking manoeuvre, both riders actually experience an increase in aerodynamic drag of the order of 6% relative to their isolated drag numbers. This type of behaviour has also been observed in the aerodynamics of racing car manoeuvres [90] and also simpler bluff body geometries such as 2D cylinders [86].

Blocken et al. [37] set out to investigate the effect of drafting on both trailing and lead riders using a full 3D CFD simulation of a multi-rider pace-line. The CFD simulations were performed for a lead and trailing rider in

Fig. 13 Smoke flow visualisation of a team pursuit team being tested in a wind tunnel

upright, drops, and aero-bar positions without the bicycle. Simulations were primarily validated by comparison to a single-rider wind tunnel set-up with limited comparison with experiments performed using a two-rider set-up. A drafting rider was found to experience both a reduction in the stagnation pressures acting on frontal surfaces and also an increase in the base pressure acting on the back. Both of these effects contributed to reductions in aerodynamic drag of a drafting rider. The magnitude of the drafting effect was dependent on rider position and varied between 27.1 and 13.8%. Compared to an isolated rider position, it was found that the relative size of the drag reduction for a trailing rider reduced for the more streamlined lower drag positions. The reported drag savings of a drafting rider are significantly lower than those found by experimental studies. It would be expected that the exclusion of the bicycle would reduce the drafting effect. Personal correspondence with the lead author of this study and unpublished results show that the exclusion of the bicycle from the simulations is likely the cause of the discrepancy between other studies that include the influence of the bicycle on the drafting effect.

The authors were also able to show that the lead rider experiences a reduction in aerodynamic drag as the spacing between the lead and trailing rider is reduced to a minimum. The reduction at the minimum gap spacing was of the order of ~ 1–3% depending on cycling position, which had not previously been reported for cyclists. In contrast to the trailing rider, when both riders were simulated in more aerodynamic positions, the magnitude of the drag reduction on the lead rider increased. The mechanism that was clearly identified by the authors was an interaction between the pressure field of the trailing rider and the base pressure of the leading cyclist. The high-pressure region generated in front of the trailing rider was found to increase the

pressure in the wake of the lead cyclist. The drafting cyclist had negligible influence on the pressure filed immediately upstream of the lead rider. This resulted in a reduction in the pressure differential between the front and back of the lead cyclist resulting in lower pressure drag which is consistent with research into other bluff bodies [86].

Additionally, Blocken and Toparlar [40] investigated the effect that a following car has on the drag of a lead cyclist—a situation one might find in a professional time-trial or in a single-rider breakaway. These authors found that the pressure field generated ahead of the vehicle was capable of reducing the rider's drag by over 10% for particularly close separation distances (less than 2 m), but even at 10 m, the effect was significant enough (0.2%) to affect the outcome of typical time-trials. More recently, Blocken et al. [41] used a similar numerical approach supported by scale model wind tunnel tests to evaluate the influence of a following motorcycle formation (up to three motorbikes). Similar to a following car, the aerodynamic effects of a close trailing motorcycle, even for relatively short following durations of a typical length road time-trial, was also found to be significant enough to dictate the outcome of the race. As a result of these findings, the authors made recommendations to the UCI to not only increase the current 10 m minimum separation distance between cars and motorcycles but also to implement measures that strictly enforce the minimum separation distance.

As the number of riders in close formation increases, the number of riding configurations and flow interactions between group members also grows in complexity. The most widely studied group formation is that of an in-line team pursuit team. Figure 14b shows the comparison of the findings of various studies into the relative power and aerodynamic drag savings of each position in the team pursuit. Despite differences in methods used to characterise
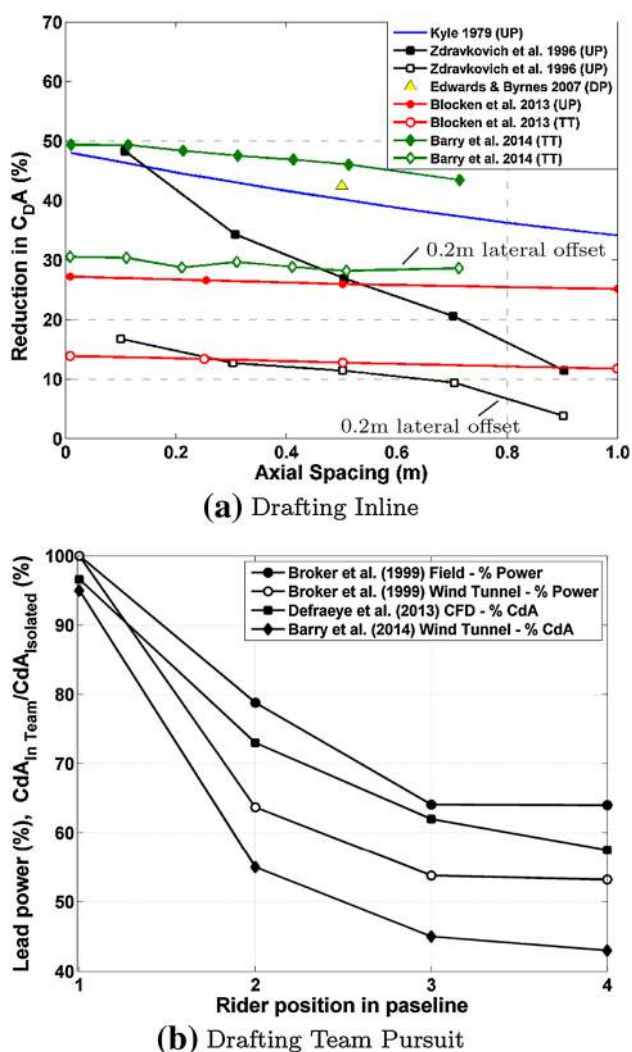
(a) Drafting Inline

(b) Drafting Team Pursuit

Fig. 14 **a** Findings from various studies investigating the influence of the drafting gap size (axial spacing) and the reduction in aerodynamic drag observed by a single trailing rider. **b** Studies showing average results for the relative power [45] and aerodynamic drag [37, 58] savings in each of the team pursuit positions one through four

the savings in each position, and the spacing between each rider, trends developed are relatively consistent among the various studies investigating drafting effects within a four-rider inline pace-line.

Broker et al. [45] in an early paper developed from team pursuit preparation for the 1996 Olympics used crank-based power meters (SRM) to measure the output of riders in a pace-line on the track. The tests were conducted in team pursuit configurations of three to four riders at an outdoor velodrome at speeds between 15.8 and 16.7 m/s, which had been estimated to be the required average speed for a winning time. Although the experimental factors, including riders' ability to hold a fixed position and maintain a constant speed while taking the lead, introduced a non-trivial level of uncertainty, the study did present a

baseline for the relative effectiveness of the different drafting positions in the team pursuit. Power measurements for each rider were normalised based on their mean power in a given position compared to their mean power while on the front. On average, for an optimised spacing between team members riders needed to produce 70.8% of their lead power in the second position and only 64.1 and 64.0% of their lead power in the third and fourth positions, respectively. The study did note substantial variability, however, due to rider position, size and mass, the order of the riders, and the drafting technique of the riders.

Recent studies by Barry et al. [58] and Defraeye et al. [38] have investigated how rider position and the ordering of athletes throughout the pace-line influence aerodynamic interactions within the team. In the wind tunnel investigations of Barry et al. [58], aerodynamic drag was measured on all four pedalling riders of a team pursuit team simultaneously to elucidate interaction effects of varying rider position. Tests were conducted whereby each rider was cycled through positions 1–4 and adopted a head-raised, lowered, tucked, and elbows together position (relative to the athlete's standard position which served as a baseline), while the remaining team assumed their standard baseline positions. Interactions were analysed by comparing measurements of each permutation to a baseline team configuration (each member holding their standard position) and with the rider's individual drag reading for each posture. Mean results showed that the riders, who were separated by 120 mm, experienced a 5, 45, 55, and 57% reduction in aerodynamic drag in positions 1–4 of the pace-line, respectively. In general, it was also found that postures that decreased the drag in individual tests will also result in a reduction in drag in the team (positions 1–4), albeit with a greater drag saving for the individual. Postures that increased individual drag also resulted in an increase in the team but with a smaller increase.

Despite these common findings, it was concluded that exactly how a change in posture would influence the aerodynamic drag of other team members was difficult to predict. It was possible to influence the aerodynamic drag of leading and trailing team members through changes in position; however, no clear relationships between the interactions evolved. This was likely due to differences between rider body position, riding style, and geometry and led the authors to conclude that the drag interactions between cyclists are athlete specific and must be treated on an individual team composition basis. Similar conclusions have also been drawn in an earlier CFD study by Defraeye et al. [38], who performed RANS simulation of four riders without bicycles modelled off of geometries from the Belgian national team. In their simulations, a narrow arm position was chosen as a baseline, and a wide arm position was chosen that increased the drag of each simulated rider

to assess the effect of a wider wake on the entire pace-line. It was noted that three of the riders had very similar measured drag area (within 2%), whereas the fourth rider had a nearly 25% greater drag area. The authors went on to show that for each of the three riders with similar drag areas, the manner in which the drag area was produced (that is, which parts of their bodies produced the most drag) varied considerably.

In the wake of reasonably well-established trends in the drafting effect on the riders in a pace-line, including the lead rider, the influence of individual rider variability is only slowly being elucidated. Despite the difficulty of developing generally applicable quantitative correlations, several robust heuristics have emerged from the last decade of multi-rider aerodynamics research:

1. The lead rider in a pace-line does experience a small reduction in drag, of the order of 5% or less compared to their baseline solo performance. This effect is a result of the high-pressure region in the front of the first trailing rider increasing the pressure in the wake of the lead rider, thereby reducing pressure drag on the lead rider [37, 38, 58].
2. The drafting effect is greater for the third rider than the second rider in a pace-line, but often remains nearly constant for subsequent riders (subject to well-matched posture and anthropometric variables). Second riders typically experience a 30–45% reduction in drag below their baseline, while subsequent riders typically experience a 35–55% reduction compared to their baselines. For riders behind the leader, not only does the wake of the rider that they are following reduce the pressure ahead of them, but the high-pressure region in front of the rider following them also reduces the pressure differential, further contributing to the total reduction in pressure drag [37, 38, 45, 53, 58, 93, 95].

6 Final remarks and areas for future research

This review presents a wide range of applied research that is important to understanding flows around cyclist geometries under racing conditions. Particularly over the past 5–10 years, advances in both experimental data acquisition and numerical modelling techniques have enabled sports aerodynamicists and researchers to develop high spatial and temporal resolution datasets of aerodynamic-related quantities. This has not only led to a greater understanding of the unsteady flow physics and aerodynamic forces in cycling but has also had a significant impact on how a practitioner in the field would approach finding solutions to cycling aerodynamic performance criteria.

Cycling is a complex aerodynamic problem and only recently have investigations focused on developing a complete picture of the flow field surrounding a cyclist. This picture has evolved, first through stationary rider investigations, then time-averaged analyses of pedalling cyclists, and more recently phase-averaged studies. Looking forward, a clearer image of the aerodynamics associated with a wider range of cycling conditions can be developed through further studies into the unsteady aerodynamics of rider position, geometry, and the motion of riders. Although the large-scale flow motions appear to be a generic feature of a wide variety of cyclist wakes, clear trends in how changes in rider position, size, shape, pedalling style, and high cadence cycling influence both the rider flow field and the aerodynamic forces are only just starting to develop.

The development and understanding of the aerodynamics of multiple riders has progressed significantly over the past decade. Current literature has focused on the aerodynamics relating to the behaviour of cooperative pace-lines, which has implications not only for team pursuits and team time-trials, but also for certain mass start situations and sprint leadout trains. In particular for the team pursuit, the teams' speed can be increased by minimising the resistance on the lead rider through interference effects which can be optimised through carefully tailoring the trailing rider's separation distance and riding position. Nonetheless, with the known importance of aerodynamics to the relative strength of both team and individual strategy within the peloton, there are still many open questions related to aerodynamics in a large amorphous pack, as well as non-steady-state aerodynamics of large groups.

At its core, cycling speed is a maximum optimisation problem between aerodynamic and biomechanical efficiency (for relatively flat terrain). Few published studies have attempted to bridge the gap between aerodynamic and biomechanical efficiency. Rider position and cycling styles are known to influence power outputs, fatigue rates, and how susceptible athletes are to injury. The influence of different riding techniques and leg kinematics throughout the stroke on both the physiology and aerodynamics of cyclists is an interesting area that warrants further research. Little is also known about the influence of the oscillatory motion of the upper body, which tends to increase with rider fatigue, on aerodynamic drag. How well the human body can adapt to aerodynamic riding positions and the best methods for achieving this in the shortest amount of time is also unclear. A greater understanding of the coupling between rider aerodynamics and biomechanics will surely lead to improved racing tactics and rider-specific training programmes with the goal of maximising both aerodynamic and physiological performance.

Just as rider position is evolving to suit the various shapes, sizes, and riding styles of athletes, so too is the development of cycling equipment. As our understanding of flows around cyclists evolves, this will impact the way cycling equipment is shaped, textured, and orientated to complement the aerodynamics of the rider. Already we are starting to see skin suits that are designed to target drag reduction on specific parts of the body based on local Reynolds numbers and helmets contoured to fit the profile of a rider's back. In industry, much of the design work of cycling equipment is initiated through numerical simulations of rider geometries holding limited static leg positions. However, we now know that the flow field changes significantly over the course of the pedal stroke. Optimised solutions for one leg position may not necessarily correlate to low time-averaged drag solutions over the course of a complete pedal stroke. Further insight into exactly how the unsteady aerodynamics associated with the movement of the legs is coupled with the aerodynamics of the bicycle frame (and vice versa) could lead to new bicycle technologies and improve the outputs of numerical and wind tunnel validation-based programmes.

To date, the vast majority of the body of literature into cycling aerodynamics has been performed in low-turbulence wind tunnels for non-yawed flow conditions with a single rider. Future aerodynamic equipment and racing postures will not only be optimised for a particular type of athlete but also for the environment in which cycling events take place. In order to achieve this, the wind environment that a cyclist and teams of riders experience on the track and road needs to be better characterised and understood. This will inform ways in which wind tunnel test methods can be improved with the goal of providing a more accurate representation of flow conditions on the race course. As wind tunnel test methods continue to evolve, the need for improved field-based measurement systems to compare with controlled wind tunnel-based findings will become even more pertinent. An improved understanding of the cycling environment under race conditions also has the potential to further inform racing rules and regulations (as has been suggested by recent publications into car and motorbike spacing between riders in road races) and the design of new indoor velodromes for increased racing speeds and spectator experience and comfort.

Numerical modelling of the flow around cyclists will continue to be an active area both in industry as a development tool and in research. Rapid growth in computing power, 3D-modelling, and scanning technologies (which also goes hand in hand with CNC and 3D printing model making for wind tunnel experiments) over the last decade has aided in simulating detailed flow fields around rider geometries for a range of cycling conditions. The wider use of CFD for research and development purposes must be accompanied with improved confidence in CFD models and also a better understanding of the limitations of numerical simulations. Accurate modelling of the transition between laminar and turbulent flow regimes, flow separation, and unsteady wakes is critical to a valid numerical simulation of flows around cyclists. If the flow physics is not being simulated, then the geometry being modelled is rendered irrelevant and so too are any numerically derived outputs. As with all CFD solutions for relatively high Reynolds numbers, errors resulting from inaccuracies in modelling the flow physics mean that validation through experiment will continue to be an integral part of any detailed CFD investigation.

One current issue with modelling separated flows around complex geometries is that simulations often involve removing certain components or significantly simplifying and smoothing the geometry to simplify the calculations. This can make it difficult to track if differences in numerical and experimental findings are a result of the different geometry, meshing characteristics, or the equations modelling the flow physics. Currently, the only way to truly determine if the flow physics have been simulated to a certain degree of accuracy is to directly compare with experimentally obtained flow fields. Validation via both experimentally obtained flow field and force datasets, and not just aerodynamic force numbers alone, will contribute to the further development of numerical simulations to better model the flow physics for a wider variety of cycling applications and the means to validate these codes. In terms of cycling CFD modelling capabilities, the next step will be to model the full dynamic motion on the legs. Due to the high computational cost of running such a simulation, it will likely be some time before full dynamic CFD solutions will be a practical method used in the optimisation of cycling aerodynamic performance.

As a final note, with many countries striving to reduce carbon emissions and traffic congestion in major cities, alternative and efficient means of commuter travel are increasingly in the spotlight. Bicycles and human-powered vehicles have been identified as an effective means to reduce the negative effects associated with fossil fuel consumption while also supporting a positive healthy and active lifestyle. As more and more people start taking up cycling-based methods of transport as a means of commuting, the effects of aerodynamics will become more important to the general population. Although this review has mainly focused on elite cycling, much of the research in this area is also applicable to commuter cycling and also more efficient means of human-powered travel such as recumbent bicycles. Findings learned from elite cycling will inevitably filter down to commuter cycling; however, since the commuter market is not dictated by racing rules

and regulations, there is far more room to move in terms of methods for aerodynamic enhancement. Aerodynamics will also be a consideration in the safe design of riding paths and rules and regulations for shared roads with cyclists and other road vehicles. The potential to improve rider performance and more generally bluff body performance through both advanced passive and active flow technologies will continue to keep aerodynamics at the forefront of cutting edge technology, research, and innovation in cycling.

References

1. Kyle CR, Bassett DR Jr (2003) The cycling world hour record. In: Burke ER (ed) High-tech cycling: the science of riding faster. Human Kinetics, Colorado, pp 175–196
2. Martin JC, Milliken DL, Cobb JE, McFadden KL, Coggan AR (1998) Validation of a mathematical model for road cycling power. J Appl Biomech 14:276–291
3. Kyle CR, Burke ER (1984) Improving the racing bicycle. Mech Eng 106(9):34–45
4. Hoerner SF (1965) Fluid-dynamic drag: practical information on aerodynamic drag and hydrodynamic resistance. Hoerner Fluid Dynamics, Midland Park, NJ
5. Munson BR, Young DF, Okiishi TH (1990) Fundamentals of fluid mechanics. New York 3:4
6. Tropea C, Yarin AL, Foss JF (2007) Springer handbook of experimental fluid mechanics. Springer, Heidelberg
7. Hucho WH (2013) Aerodynamics of road vehicles: from fluid mechanics to vehicle engineering. Elsevier, Cambridge
8. Gibertini G, Grassi D (2008) Cycling aerodynamics. In: Nørstrud H (ed) Sport aerodynamics, vol 506. Springer, Vienna, pp 23–47
9. Martin JC, Davidson CJ, Pardyjak ER (2007) Understanding sprint-cycling performance: the integration of muscle power, resistance, and modeling. Int J Sports Physiol Perform 2(1):5
10. Bearman PW (1997) Near wake flows behind two-and three-dimensional bluff bodies. J Wind Eng Ind Aerodynam 69:33–54
11. Schlichting H (1968) Boundary-layer theory. McGraw-Hill, New York
12. Crouch TN, Burton D, Brown NAT, Thompson MC, Sheridan J (2014a) Flow topology in the wake of a cyclist and its effect on aerodynamic drag. J Fluid Mech 748:5–35
13. Crouch TN, Burton D, Thompson MC, Brown NAT, Sheridan J (2016) Dynamic leg-motion and its effect on the aerodynamic performance of cyclists. J Fluids Struct 65:121–137
14. Griffith MD, Crouch TN, Thompson MC, Burton D, Sheridan J, Brown NAT (2014) Computational fluid dynamics study of the effect of leg position on cyclist aerodynamic drag. J Fluids Eng 136(10):101105
15. Kyle CR, Brownlie LW, Harber E, MacDonald R, Norstrom M (2004) The nike swift spin cycling project: reducing the aerodynamic drag of bicycle racing clothing by using zoned fabrics. Eng Sport 5:1
16. Crouch TN, Burton D, Thompson MC, Martin DT, Brown NAT, Sheridan J (2014) A phase-averaged analysis of the pedalling cyclist wake. In: 19th Australasian Fluid Mechanics Conference (Melbourne, Australia 8-11 December 2014). RMIT University, pp 1–4
17. Baidya R, Monty JP, Hutchins N (2010) Aerodynamics of high cadence cycling. In: 17th Australasian Fluid Mechanics Conference (Auckland, New Zealand 5–9 December 2010). Melbourne University, pp 1–4
18. Andrew JB (2013) Specialized builds its own wind tunnel. http://www.bicycling.com/bikes-gear/reviews/specialized-builds-its-own-wind-tunnel. Accessed 2 Mar 2016
19. Wordley S, Saunders JW (2008) On-road turbulence. SAE Int J Passenger Cars Mech Syst 1(2008-01-0475):341–360
20. Wordley S, Saunders JW (2009) On-road turbulence: Part 2. SAE Int J Passenger Cars Mech Syst 2(2009-01-0002):111–137
21. Maskell EC (1963) A theory of the blockage effects on bluff bodies and stalled wings in a closed wind tunnel. Technical report, DTIC Document
22. Awbi HB (1978) Wind-tunnel-wall constraint on two-dimensional rectangular-section prisms. J Wind Eng Ind Aerodynam 3(4):285–306
23. Mercker E, Wiedemann J (1996) On the correction of interference effects in open jet wind tunnels. SAE Paper 105(6):795–809
24. Cooper K (1998) Bluff-body blockage correction in closed and open test section wind tunnels. AGARD, AG-336, NTIS, Springfield, VA, p 6
25. Chabroux V, Mba MN, Sainton P, Favier D (2010) Wake characteristics of time trial helmets using piv-3c technique. In: 15th Int. Symp. on Applications of Laser Techniques to Fluid Mechanics, Lisbon, Portugal, vol 58
26. Brownlie L, Kyle C, Carbo J, Demarest N, Harber E, MacDonald R, Nordstrom M (2009) Streamlining the time trial apparel of cyclists: the nike swift spin project. Sports Technol 2(1–2):53–60
27. Defraeye T, Blocken B, Koninckx E, Hespel P, Carmeliet J (2010a) Computational fluid dynamics analysis of cyclist aerodynamics: performance of different turbulence-modelling and boundary-layer modelling approaches. J Biomech 43(12):2281–2287
28. Debraux P, Grappe F, Manolova AV, Bertucci W (2011) Aerodynamic drag in cycling: methods of assessment. Sports Biomech 10(3):197–218
29. Heil D (2001) Body mass scaling of projected frontal area in competitive cyclists. Eur J Appl Physiol 85(3–4):358–366
30. Heil DP (2002) Body mass scaling of frontal area in competitive cyclists not using aero-handlebars. Eur J Appl Physiol 87(6):520–528
31. Dorel S, Hautier CA, Rambaud O, Rouffet D, Van Praagh E, Lacour JR, Bourdin M (2005) Torque and power-velocity relationships in cycling: relevance to track sprint performance in world-class cyclists. Int J Sports Med 26(9):739–746
32. Barlow JB, Rae WH, Pope A (1999) Low-speed wind tunnel testing, 3rd edn. Wiley, New York
33. Hanna RK (2002) Can CFD make a performance difference in sport. Eng Sport 4:17–30
34. Godo MN, Corson D, Legensky SM (2009) An aerodynamic study of bicycle wheel performance using CFD. In: 47th AIAA Aerospace Sciences Annual Meeting, Orlando, FL, USA, pp 5–8
35. Godo MN, Corson D, Legensky SM (2010) A comparative aerodynamic study of commercial bicycle wheels using CFD. AIAA Paper, pp 2010–1431
36. Defraeye T, Blocken B, Koninckx E, Hespel P, Carmeliet J (2011) Computational fluid dynamics analysis of drag and convective heat transfer of individual body segments for different cyclist positions. J Biomech 44(9):1695–1701

37. Blocken B, Defraeye T, Koninckx E, Carmeliet J, Hespel P (2013) CFD simulations of the aerodynamic drag of two drafting cyclists. Comput Fluids 71:435–445

38. Defraeye T, Blocken B, Koninckx E, Hespel P, Verboven P, Nicolai B, Carmeliet J (2014) Cyclist drag in team pursuit: influence of cyclist sequence, stature, and arm spacing. J Biomech Eng 136(1):011005

39. Tu J, Yeoh GH, Liu C (2012) Computational fluid dynamics: a practical approach. Butterworth-Heinemann, Oxford

40. Blocken B, Toparlar Y (2015) A following car influences cyclist drag: CFD simulations and wind tunnel measurements. J Wind Eng Ind Aerodyn 145:178–186

41. Blocken B, Toparlar Y, Andrianne T (2016) Aerodynamic benefit for a cyclist by a following motorcycle. J Wind Eng Ind Aerodyn 155:1–10

42. Defraeye T, Blocken B, Koninckx E, Hespel P, Carmeliet J (2010b) Aerodynamic study of different cyclist positions: CFD analysis and full-scale wind-tunnel tests. J Biomech 43(7):1262–1268

43. Fintelman DM, Hemida H, Sterling M, Li F-X (2015a) CFD simulations of the flow around a cyclist subjected to crosswinds. J Wind Eng Ind Aerodyn 144:31–41

44. Lukes RA, Hart JH, Chin SB, Haake SJ (2005) The role and validation of CFD applied to cycling. In: Fluent user group meeting. Fluent, pp 65–75

45. Broker JP, Kyle CR, Burke ER (1999) Racing cyclist power requirements in the 4000-m individual and team pursuits. Med Sci Sports Exerc 31(11):1677–1688

46. Blair K, Chew GL, Cote M (2007) The effect of static leg position and cadence on the drag of a cyclist. Hum Power eJ 4:1–3

47. Fintelman DM, Sterling M, Hemida H, Li F-X (2015b) The effect of time trial cycling position on physiological and aerodynamic variables. J Sports Sci 33(16):1730–1737

48. Fintelman DM, Sterling M, Hemida H, Li FX (2015) Effect of different aerodynamic time trial cycling positions on muscle activation and crank torque. Scand J Med Sci Sports

49. Underwood L, Schumacher J, Burette-Pommay J, Jermy M (2011) Aerodynamic drag and biomechanical power of a track cyclist as a function of shoulder and torso angles. Sports Eng 14(2–4):147–154

50. Candau RB, Grappe F, Ménard M, Barbier B, Millet GY, Hoffman MD, Belli AR, Rouillon JD (1999) Simplified deceleration method for assessment of resistive forces in cycling. Med Sci Sports Exerc 31(10):1441–1447

51. García-López J, Rodríguez-Marroyo JA, Juneau CE, Peleteiro J, Martínez AC, Villa JG (2008) Reference values and improvement of aerodynamic drag in professional cyclists. J Sports Sci 26(3):277–286

52. Kawamura TM (1953) Wind drag of bicycles. Tokyo University, Tokyo

53. Zdravkovich MM, Ashcroft MW, Chisholm SJ, Hicks N (1996) Effect of cyclists' posture and vicinity of another cyclists on aerodynamic drag. Eng Sport 1:21–28

54. Padilla S, Mujika I, Angulo F, Goiriena JJ (2000) Scientific approach to the 1-h cycling world record: a case study. J Appl Physiol 89(4):1522–1527

55. Barry N, Burton D, Sheridan J, Thompson MC, Brown NAT (2014) Aerodynamic performance and riding posture in road cycling and triathlon. In: Proceedings of the Institution of Mechanical Engineers, Part P: Journal of Sports Engineering and Technology, pp 1–11

56. Davies CTM (1980) Effect of air resistance on the metabolic cost and performance of cycling. Eur J Appl Physiol Occup Physiol 45(2–3):245–254

57. Jeukendrup AE, Martin J (2001) Improving cycling performance: how should we spend our time and money. Sports Med 31(7):559–569

58. Barry N, Burton D, Sheridan J, Thompson MC, Brown NAT (2015) Aerodynamic drag interactions between cyclists in a team pursuit. Sports Eng 18(2):93–103

59. Jr Bassett DR, Kyle CR, Passfield L, Broker JP, Burke ER, Burke ER (1999) Comparing cycling world hour records, 1967–1996: modeling with empirical data. Med Sci Sports Exerc 31(11):1665–1676

60. McLean BD, Danaher R, Thompson L, Forbes A, Coco G (1994) Aerodynamic characteristics of cycle wheels and racing cyclists. J Biomech 27(6):675–675

61. Broker JP (2003) Cycling power: road and mountain. In: Burke ER (ed) High-tech cycling: the science of riding faster. Human Kinetics, Colorado, pp 147–174

62. Kyle CR (2003) Selecting cycling equipment. In: Burke ER (ed) High-tech cycling: the science of riding faster. Human Kinetics, Colorado, pp 1–48

63. Blair KB, Sidelko S (2008) Aerodynamic performance of cycling time trial helmets. Eng Sport 7:371–377

64. Chabroux V, Barelle C, Favier D (2008) Aerodynamics of time trial bicycle helmets. Eng Sport 7:401–410

65. Parker BA, Franke ME, Elledge AW (1996) Bicycle aerodynamics and recent testing. In: 34th AIAA aerospace sciences meeting, Reno, NV, 15–18 Jan 1996

66. Bearman PW, Morel T (1983) Effect of free stream turbulence on the flow around bluff bodies. Prog Aerospace Sci 20(2):97–123

67. ABC (2012) Bobridge blown off his bike. http://www.abc.net.au/news/2012-01-11/bobridge-blown-off-his-bike/3767346. Accessed 10 May 2016

68. Birnie L (2010) Giro analysis: Crosswinds and crashes cause chaos in holland. http://www.cyclingweekly.co.uk/news/racing/giro-ditalia/giro-analysis-crosswinds-and-crashes-cause-chaos-in-holland-61064. Accessed 25 Mar 2016

69. Cyclingtips Marino M (2016) Project 2016: The story behind usa cyclings revolutionary new track bikes. http://cyclingtips.com/2016/05/project-2016-the-story-behind-usa-cyclings-revolutionary-new-track-bikes/. Accessed 17 June 2016

70. Zdravkovich MM (1992) Aerodynamics of bicycle wheel and frame. J Wind Eng Ind Aerodyn 40:55–70

71. Approval protocol for frames and forks (2016) Union Cycliste Internationale

72. Clarification guide of the uci technical regulation, 15.01.2016 version (2016). Union Cycliste Internationale

73. Tew GS, Sayers AT (1999) Aerodynamics of yawed racing cycle wheels. J Wind Eng Ind Aerodyn 82:209–222

74. Godo MN, Corson D, Legensky SM (2011) A practical analysis of unsteady flow around a bicycle wheel, fork and partial frame using CFD. In: 49th AIAA Aerospace Sciences Meeting including the New Horizons Forum and Aerospace Exposition, pp 1237

75. Sidelko S (2007) Benchmark of aerodynamic cycling helmets using a refined wind tunnel test protocol for helmet drag research. PhD thesis, Massachusetts Institute of Technology

76. Brownlie L, Ostafichuk P, Tews E, Muller H, Briggs E, Franks K (2010) The wind-averaged aerodynamic drag of competitive time trial cycling helmets. Procedia Eng 2(2):2419–2424

77. Achenbach E (1971) Influence of surface roughness on the cross-flow around a circular cylinder. J Fluid Mech 46(02):321–335

78. Fage A, Warsap JH (1930) The effects of turbulence and surface roughness on the drag of a circular cylinder. HM Stationery Office, London

79. Brownlie LW (1992) Aerodynamic characteristics of sports apparel. PhD thesis, Theses (School of Kinesiology)/Simon Fraser University

80. Oggiano L, Troynikov O, Konopov I, Subic A, Alam F (2009) Aerodynamic behaviour of single sport jersey fabrics with different roughness and cover factors. Sports Eng 12(1):1–12

81. Oggiano L, Brownlie L, Troynikov O, Bardal LM, Sæter C, Sætran L (2013) A review on skin suits and sport garment aerodynamics: guidelines and state of the art. Proced Eng 60:91–98

82. Bardal LM, Oggiano L, Sætran L, Konopov I, Troynikov O (2011) Comparison of aerodynamic properties of wool and polyester knitted textiles. Proced Eng 13:363–369

83. Underwood L, Jermy MC (2011) Fabric testing for cycling skinsuits. Proced Eng 13:350–356

84. DAuteuil A, Larose GL, Zan SJ (2010) Relevance of similitude parameters for drag reduction in sport aerodynamics. Proced Eng 2(2):2393–2398

85. Chowdhury H, Alam F, Subic A (2010) Aerodynamic performance evaluation of sports textile. Proced Eng 2(2):2517–2522

86. Biermann D, Herrnstein WH Jr (1934) The interference between struts in various combinations. National Advisory Committee for Aeronautics, Technical Report 468

87. Zdravkovich MM (1977) Review of flow interference between two circular cylinders in various arrangements. J Fluids Eng 99(4):618–633

88. Kim MK, Kim DK, Yoon SH, Lee DH (2008) Measurements of the flow fields around two square cylinders in a tandem arrangement. J Mech Sci Technol 22(2):397–407

89. Martinuzzi RJ, Havel B (2004) Vortex shedding from two surface-mounted cubes in tandem. Int J Heat Fluid Flow 25(3):364–372

90. Romberg GF, Chianese F, Lajoie RG (1971) Aerodynamics of race cars in drafting and passing situations. Technical report, SAE Technical Paper

91. Zabat M, Frascaroli S, Browand FK (1994) Drag measurements on 2, 3 and 4 car platoons. Technical report, SAE Technical Paper

92. Watkins S, Vino G (2008) The effect of vehicle spacing on the aerodynamics of a representative car shape. J Wind Eng Ind Aerodyn 96(6):1232–1239

93. Barry N, Burton D, Sheridan J, Thompson M, Brown NAT (2016) Flow field interactions between two tandem cyclists. Exp Fluids 57(12):181

94. Kyle CR (1979) Reduction of wind resistance and power output of racing cyclists and runners travelling in groups. Ergonomics 22(4):387–397

95. Barry N, Sheridan J, Burton D, Brown NAT (2014) The effect of spatial position on the aerodynamic interactions between cyclists. Proced Eng 72:774–779

96. Edwards AG, Byrnes WC (2007) Aerodynamic characteristics as determinants of the drafting effect in cycling. Med Sci Sports Exerc 39(1):170–176. doi:10.1249/01.mss.0000239400.85955.12